Experimental Testbed for Load Control on an AC/DC Microgrid

A Thesis

Submitted to the Faculty

of

Drexel University

by

Edwin J. John

in partial fulfillment of the

requirements for the degree

of

Master of Science in Electrical Engineering

September 2017

ACKNOWLEDGMENTS

TABLE OF CONTENTS

LIST OF TABLES

LIST OF FIGURES

ABSTRACT

Experimental Testbed for Load Control on an AC/DC Microgrid
Edwin J. John
Karen Miu, Ph.D.

Microgrids are becoming increasingly popular in the world of power systems to mitigate the effects of high impact events that can lead to blackouts. They are also integral to including distributed renewable energy generation in the grid. A major challenge in effective implementation of DC microgrids, in particular, is the lack of adequate testing platforms. This thesis primarily aims to build a testbed of an AC/DC microgrid in a laboratory environment using programmable sources and loads. A central measurement and control platform is developed to monitor and actuate all the loads from a single unit. While this enhances data measurement, it also enables simultaneous operation of the loads. The use of such state-of-the-art technology gives a better understanding of integration of microgrids into existing power systems.

Having a microgrid testbed allows for the study of the control of hybrid AC/DC microgrids under various operating conditions. This thesis uses this capability to test a load shedding problem on a 3 bus and 4 bus AC/DC microgrid. An algorithmic solution to the problem is proposed and implemented in hardware. The results are compared to more traditional control strategies. The microgrid testbed developed in this thesis can prove integral to future research work on AC/DC microgrid controllers. The central control platform can also be used for future research into the effect of communication networks on the performance of the microgrid and power system as a whole.

1. INTRODUCTION

1.1. OVERVIEW

Power systems today face a major increase in loading, according to the International Energy Agency [32], while still increasingly dependent on generation sources that are located remotely from load centers, making them much more prone to voltage collapses than in the previous century. This makes way for the introduction of microgrids into an already complex grid. Microgrids have power generation capabilities at various distributed locations in the grid and so alleviate the demand on central generating stations. They also have the ability to implement both source and load control for both an efficient and smarter utilization of resources. DC Microgrids are becoming increasingly popular due to the advancements in energy storage devices and renewable sources of power. Most renewable energy sources generate DC power and even most modern loads are moving towards DC loading. This reduces the losses in transmission and also reduces the need for power electronic drives.

This thesis focused on developing a centrally monitored and controlled hybrid AC/DC microgrid testbed. Programmable sources and loads are used to build a highly flexible and reconfigurable hardware setup in Drexel University's Center for Electric Power Engineering. A central monitoring and control interface was developed that can measure and actuate the loads in real time. This laboratory testbed is then used to implement and study load control by taking into account the various types of loads.

In this chapter, the following topics are presented:

- A background and motivation for the work;

- A list of objectives and a summary of contributions;

- An overview of the thesis organization.

1.2. BACKGROUD AND MOTIVATION

The power grid has traditionally been dominated by AC transmission and loads ever since Westinghouse and Tesla won the "war of currents" over 100 years ago [22]. The invention of transformers won the battle for alternating currents, and the advantages gained from an AC transmission system have dominated over its weaknesses. Commercial applications and other loads were forced to adapt to an AC supply while direct currents and its possibilities were limited to research and experiments. In the last 50 years, however, factors such as advanced power electronics, penetration of renewable power sources into distribution systems, and an increasing complexity of the grid due to loads being integrated through embedded AC/DC converters have brought about a rethink of roles of DC and AC, especially in distribution systems.

Recently, researchers have proposed a hybrid AC and DC grid at distribution levels. This concept is built on the advantages individual AC and DC grids cannot provide such as directly integrating AC/DC loads and renewable sources to AC/DC links respectively. Eliminating multiple DC-AC-DC and AC-DC-AC conversions increases system efficiency, while decreasing complexity and associated costs [21]. Figure 1.1 shows a

hybrid AC/DC microgrid proposed by the authors of [21]. While this was proposed as a future grid solution, such a system consists of both AC and DC distribution networks connected through a three-phase AC/DC converter. Multiple renewable energy resources are integrated into the system both on the AC and DC side while multiple conversions to operate different loads are kept to a minimum. The AC side of the distribution system can also be connected to the utility grid through a transformer.
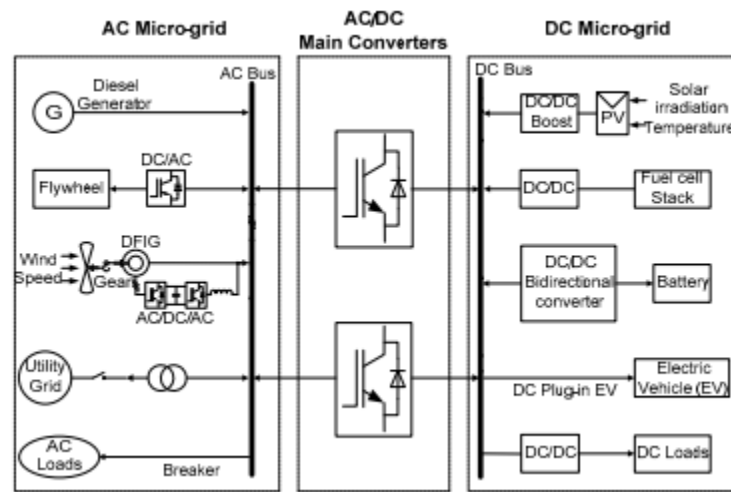
Figure 1.1 A Hybrid AC/DC Microgrid System

Numerous efforts have been made all over the world to study and examine microgrids through laboratory testbeds or simulations [23,24]. Since there is no particularly accepted benchmark test system, different microgrid topologies have been explored by researchers and even commercially implemented. Since the design of microgrids can be very versatile, the objectives, usage and results obtained have been wide-ranging [25,26]. There is still no standard voltage level for the DC grid and while a DC microgrid requires only voltage stabilization, the protection system of DC distribution system is not matured enough [28] compared to the AC system. Building an actual testbed in an experimental environment allows the interconnection of the various components depicted in Figure 1.1

and the ability to experiment on them. The Consortium for Electric Reliability Technology Solutions (CERTS) is one of the most renowned microgrid projects in the U.S. [28], while countries like China [29], Australia [30] and Spain [31] have also forayed into building testbeds for research purposes. Institutional microgrid testbeds similar to the one developed in this thesis are discussed in detail in Chapter 2.

This thesis uses programmable sources and loads to build an experimental AC/DC microgrid testbed with the aim of being able to continuously monitor and actuate the loads from a central control unit. Subsequently the testbed is used to investigate extreme loading conditions on the DC microgrid and the effectiveness of different voltage control strategies. An AC/DC microgrid testbed is also a valuable tool for other research activities in the center.

1.3. OBJECTIVES

The objectives of this thesis include:

- Investigating existing experimental microgrid testbeds. Distinguishing factors were determined to be:

    - Programmable source and loads

    - Central monitoring and control center

- Constructing a hybrid AC/DC microgrid testbed using programmable sources and loads which can achieve the following:

    - Simulate different sources present in a microgrid such as distributed generators, renewable energy and storage systems

- Emulate different loading conditions with a capability of mimicking unstable loading conditions in a safe and controlled laboratory environment

- Building a central monitoring and control center allowing the user to efficiently supervise the system measurements, establish the quality of these measurements by referencing against a calibrated power analyzer and actuate the loads in times of loading issues based on these measurements

- Testing different load control strategies with an aim of mitigating undervoltage conditions through load shedding.

Figure 1.2 graphically shows the thesis' framework: the focus of this thesis is on the development of a microgrid testbed that can be used to test different AC/DC microgrid architectures. A major distinguishing aspect of the testbed is the use of programmable loads to simulate different load types, and its operation is briefly reviewed in Chapter 3. The instrumentation and measurement system in the microgrid testbed allows for continuous monitoring of the system and implementation of various control algorithms. A load control algorithm is proposed in this thesis to mitigate an overloading condition through load shedding. Some background work done for this thesis included studying microgrid structures with a focus on laboratory testbed implementations to be able to improve upon status quo.
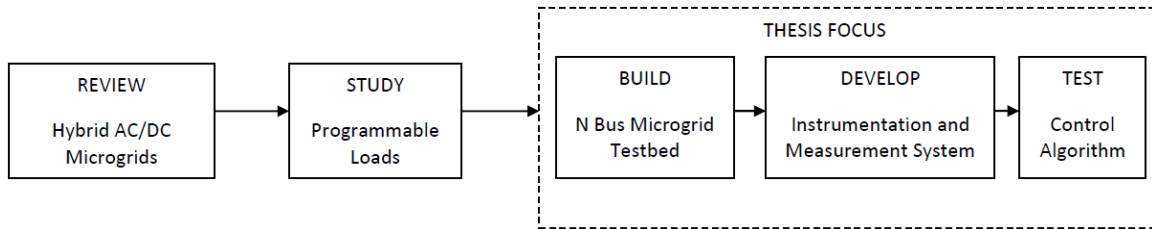
Figure 1.2 Graphical Representation of Thesis Framework

1.4. SUMMARY OF CONTRIBUTIONS

The thesis' contributions are summarized here:

- Development of a hybrid AC/DC microgrid testbed that integrates various state-of-the-art equipment in the power laboratory including programmable source, programmable loads and a multi-channel power analyzer.

- Describing the expansion of the testbed to an N bus system to obtain a highly reconfigurable setup that can be tailored for different research to test various ideas and concepts.

- Development of a software tool that acts as a central monitoring and control platform for the programmable loads in the testbed.

- Formulation of a load shedding problem:
    - Given: estimated amount of voltage to be recovered to reach an acceptable voltage threshold value
    - Determine: load control strategy that
        - Brings the bus voltage within a tolerance of the desired threshold value

- Effectiveness of different solutions compared through achieving the result with a minimal power metric of percentage change in power delivered to each of the loads operating on the bus

- Experimental results of load control strategies that consider ZIP loads as individual loads having different voltage sensitivities instead of executing load shedding on them as aggregate loads.

1.5. ORGANIZATION OF THESIS

This thesis is organized as follows:

- In Chapter 2, the development of an experimental DC microgrid testbed in a laboratory environment is detailed, explaining the selection of components to move from a three-bus system to four bus system, and how they relate to a real world microgrid.

- In Chapter 3, the software aspect is covered i.e. the central measurement and control interface for the programmable loads built on a National Instruments LabVIEW platform.

- In Chapter 4, a load shedding problem is discussed and select control algorithms are compared and formulated. Test results and evaluation of the proposed methodologies are also presented.

- Finally, in Chapter 5, the research accomplishments and contributions of this particular thesis are summarized, and a discussion of the future work and prospects of the setup is proposed.

2. LABORATORY SETUP OF THE EXPERIMENTAL TESTBED

2.1. OVERVIEW

DC Microgrids are gaining popularity in an electric power system that is continuously trying to improve efficiency and reliability. Power systems as a whole are designed and built to be highly reliable. However, many high impact and less frequent events such as a natural disaster or a blackout has called for a self-healing capability. This can be provided by microgrids.

According to the U.S. Department of Energy, "a microgrid is a group of interconnected loads and distributed energy resources within clearly defined electrical boundaries that acts as a single controllable entity with respect to the grid and that connects and disconnects from such grids to enable it to operate in both grid-connected or island mode" [9]. This has put a focus on the design and control of such microgrids.

A DC microgrid is better suited to provide the advantages that are expected of a microgrid since many of the distributed resources involve renewable DC energy and battery storage while most modern DC loads require additional AC/DC or DC/AC converters if they are to be connected to an AC grid. This reverse conversion results in loss of efficiency. In a DC microgrid, on the other hand, the number of power conversions required for connecting DC loads is significantly reduced to enhance system energy efficiency [10,11]. There are fewer documented commercial implementations of - or research done on - DC microgrids as compared to AC microgrids. However, advancements

in semiconductor technology and increasingly efficient power electronic converters have brought about a renewed interest in DC microgrids. The major challenge that a DC microgrid faces is an effective control design in order to maintain stability in adverse conditions. Thus, a microgrid testbed is a valuable tool in understanding the effects of integration of a DC microgrid into existing power systems.

Many institutions have developed such a hardware testing platform such as the Microgrid testbed at Penn State Harrisburg that has three electrical buses – an AC source bus which is connected to the utility grid, and DC buses acting either as a storage bus or as a load bus. It has a total power capability of 12kW [14]. The City College of New York built a DC microgrid which is connected to the utility grid through converters and also has two 6kW programmable DC photovoltaic power emulators. It has a single central DC bus, to which a battery storage system and an AC/DC load emulation system is connected [13].

This thesis introduces a hardware experimental testbed of a 4 bus AC/DC microgrid in the Center for Electric Power Engineering laboratory in Drexel University. The objective of the setup is to have a testing platform to understand the operation and control of AC/DC microgrids under a variety of conditions. A combination of AC and DC sources supplying a high number of DC loads represents a very common setting in power systems. Building an actual microgrid setup in a laboratory environment will present a reconfigurable system in which different operational scenarios and control schemes can be implemented.

The proposed hybrid AC/DC microgrid helps mitigate the issues raised in [11] and facilitates interconnection of various AC/DC source and loads to the power system while reducing multiple reverse conversions present in an individual AC or DC microgrid [12]. Some of the characteristics of the testbed presented in this thesis are as follows:

i.   An ability to run transmission line and loading experiments using actual components giving a better understanding of overloading issues as well as breakdown points as opposed to simulations,

ii.   Source emulation capability achieved using Chroma 61511 programmable source; thus, mimicking different sources used in everyday life such as diesel generators, renewable energy sources like wind and solar, or a battery and inverter combination,

iii. Load programming capability achieved using Chroma programmable loads on the DC buses to emulate modern loads which run on DC power - these loads are programmed to emulate different load models to match different loading scenarios and this helps in studying the effect of DC loads on the microgrid – and,

iv.   A central monitoring and control station to capture and to actuate different events such as contingencies and the effects of corresponding corrective measures. It also enables testing and implementing different AC/DC microgrid control techniques.

The hardware setup detailed in the following sections uses a programmable AC source which feeds a three-phase rectifier through a transmission line to create a DC source at that bus. A DC microgrid is then created by adding an additional line, bus and loads so that the final setup is a hybrid AC/DC microgrid. Programmable DC loads are used to setup and test both a three bus and a four bus microgrid architecture. The test platform does allow for microgrids with a large number of buses.

The controllable loads allow the study of the effects of different types of loading on voltage regulation of the microgrid. Two different models are described in Section 2.2 and 2.3 with an additional DC bus being introduced in Section 2.3. Once the setup is operational, different control techniques are used for the two setups in order to mitigate an overloading condition through load shedding. The control approach is described in detail in Chapter 4.

2.2. THREE BUS SYSTEM

Before building the complete 4 bus AC/DC microgrid, it is desired to look at the setup progressively. A DC bus is branched out from a traditional 2 bus AC power system using a converter. This gives us a 3 bus system as described in Figure 2.1. The main purpose of building this configuration is to understand the feasibility of building a successful model that can address a range of loading conditions including heavy loading conditions and, subsequently, voltage regulation.
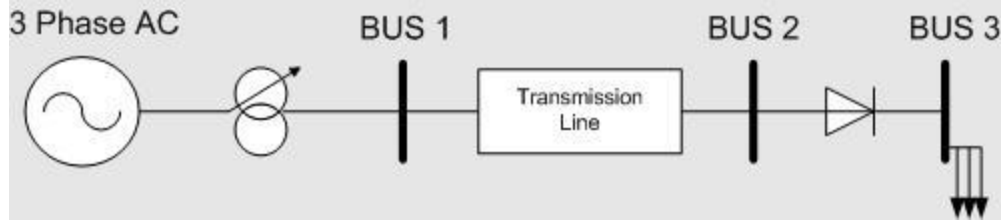
Figure 2.1 Single Line Diagram of Test Setup 1

The AC grid in Figure 2.1 is a standard two bus power system with a reactive transmission line carrying the three-phase power. For this thesis, only DC loads are considered and so there are no loads connected to the AC part of the microgrid. A three-phase programmable AC source at Bus 1 is the source of power in the setup as shown in Figure 2.1. This programmable source is powered by a fixed three-phase utility supply. Using a Chroma programmable source gives us the flexibility to mimic different renewable energy sources by changing the power factor and adding different DC offsets. It uses advanced PWM technology to set a slew rate for the voltage and frequency. For the scope of this thesis however, this source is set to act as an ideal $208V_{LL}$ AC source with a power rating of 12kVA.

The autotransformer is used to maintain a $120V_{DC}$ voltage level at Bus 3. The AC bus is connected to a three-phase diode rectifier through a transmission line hardware model which is set at 6Ω reactance per phase. The line reactance is modelled on an in-house simulated transmission line module [1], that was built to resemble a π-model of a transmission line using lumped parameter equipment. The hardware setting line reactance is chosen to represent a short length transmission line but this can easily be changed. While

the line reactance setting can be modified with ease to serve as a medium or long length transmission line by changing the value of the π-model components, shorter length lines are more representative of microgrid line parameters (i.e. no line charging).

The converter used in this thesis is a three-phase full wave diode rectifier which rectifies the AC and gives a DC voltage of magnitude determined by

$$V_{dc} = \frac{3\sqrt{2}}{\pi} V_{LL}$$

The converter characteristics are assumed to be fixed and it generates a standard rectified DC voltage.
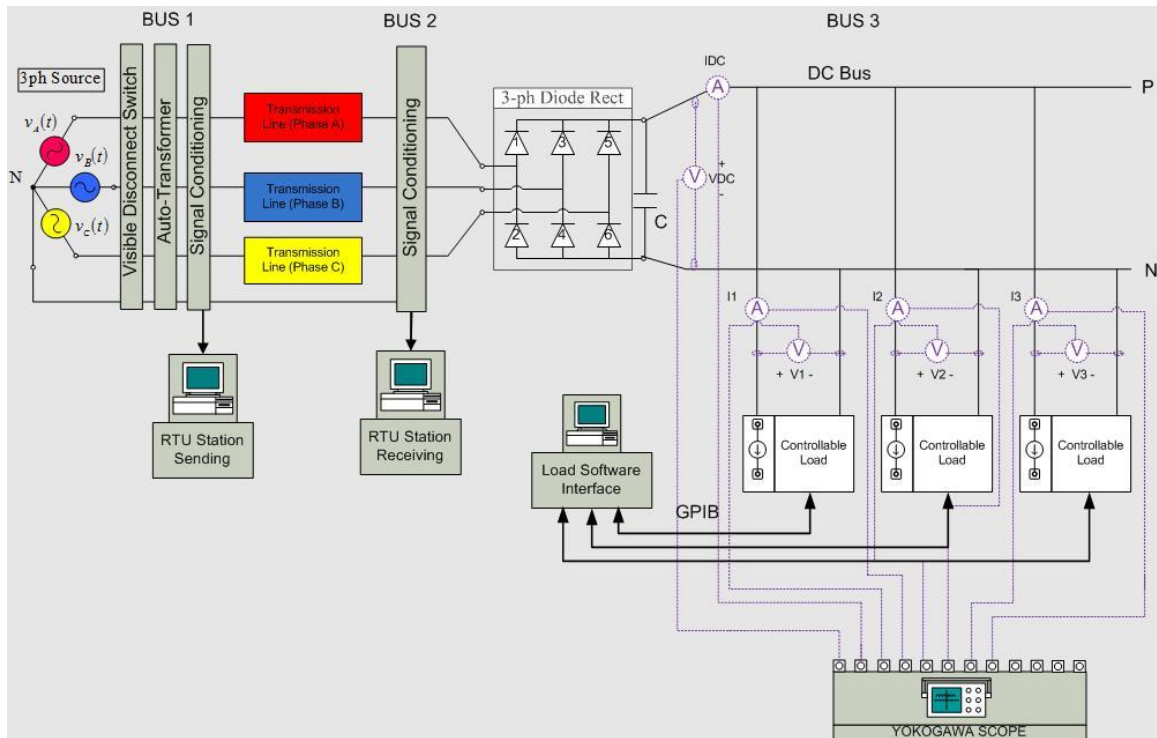
Figure 2.2 Circuit Diagram of 3 Bus System

The rectified DC voltage is filtered through a 1800uF Aluminum electrolytic capacitor in order to smoothen the voltage profile. The capacitor is connected across the positive and negative terminals of Bus 3. The capacitor shorts the higher frequency AC ripples to the ground by providing a lower resistance path and blocks the lower frequency pure DC components so that it flows through to the DC bus. It is used to provide a smoother voltage profile to the electronic DC loads.

2.3. FOUR BUS SYSTEM

A fourth bus is added to the three-bus system developed so as to have a DC grid in addition to the AC grid. This leads to the entirety of the AC/DC microgrid structure presented in this thesis with two AC buses carrying no loads and two DC buses each supplying some load. A reactive transmission line is introduced in the phase line between Bus 3 and Bus 4 as shown in the single line diagram in Figure 2.3. One of the DC loads is then shifted to Bus 4 while the other two remain at Bus 3. The autotransformer continues to be regulated to maintain the voltage at Bus 3 to be $120V_{DC}$ leading to a slightly lower nominal voltage at Bus 4.
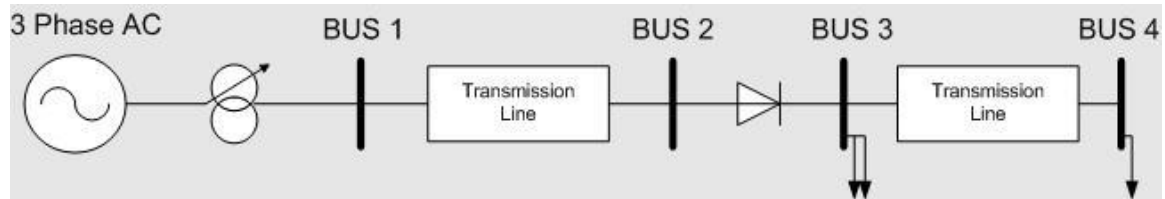
Figure 2.3 Single Line Diagram of Test Setup 2

The circuit for the AC/DC microgrid is setup as shown in Figure 2.4. It is similar to the first test setup except that Bus 4 is connected to Bus 3 through an equivalent series distribution line impedance. The DC line model is composed of the mostly reactive transmission line module [1] in series with an adjustable resistive load bank. Most overhead and especially underground distribution lines have a higher R/X ratio compared to transmission lines such as the one between Bus 1 and Bus 2. An equivalent series line model is representative of such a DC distribution line within the microgrid.

The resistive load bank used in the testbed has a rating of 10kW at $200V_{DC}$. It consists of series and parallel combination of rheostats that allows for coarse and fine adjustment of resistances. The resistance value is controlled locally and individual rheostats can be excluded from the circuit using breakers. The current through and voltage across the load bank is displayed on a digital ammeter and digital voltmeter respectively. While the resistance setting can be changed easily, an arbitrary resistance of 6Ω is set for the tests conducted in this thesis. This gives an effective phase impedance of a transmission line box reactance of 6Ω and a resistive line of 4Ω. One Chroma programmable load is now being supplied by this new bus while the other two remain at Bus 3.
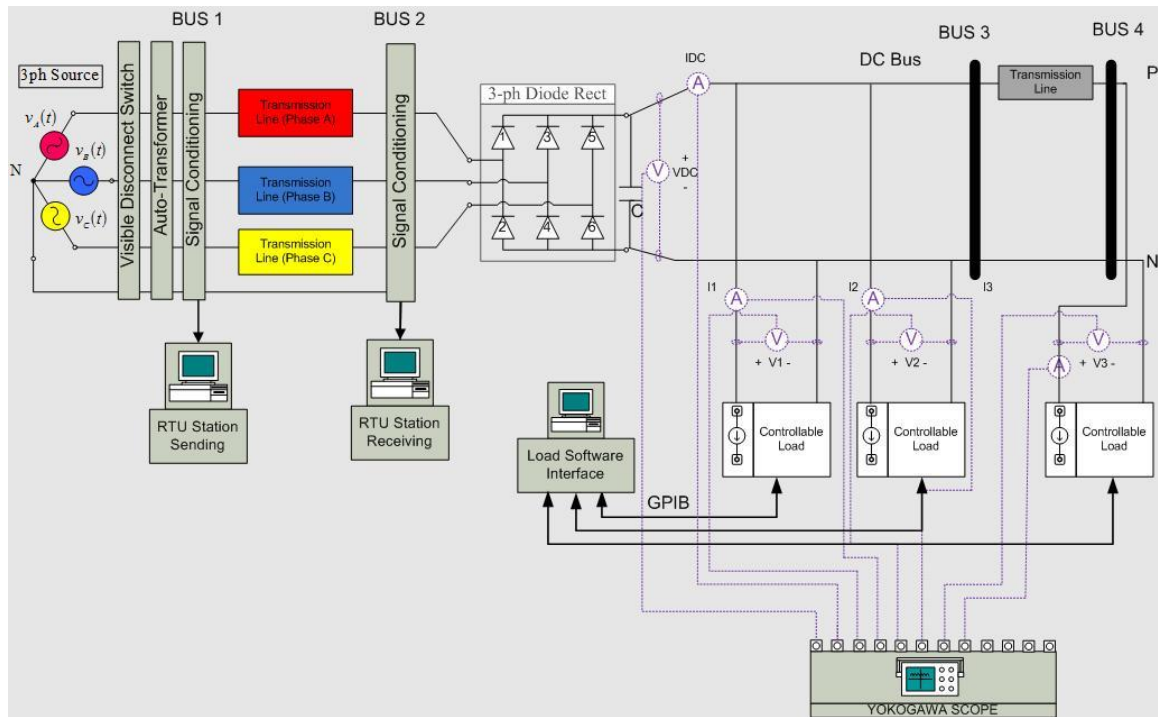
Figure 2.4 Circuit Diagram of 4 Bus System

The power system drawn out in Figure 2.4 was physically setup in the Drexel power laboratory. In Figure 2.5 below, the PECO power supply is located on the main transfer panel (back, center). The Chroma programmable source (front left) is powered from the panel and is in turn connected to the three-phase autotransformer (back left) to control the magnitude of voltage being transmitted. The two signal conditioning boxes are continuously measuring the AC current and voltage on either side of the three-phase transmission line between Bus 1 and Bus 2 (front center) and can be viewed on the remote terminal units.
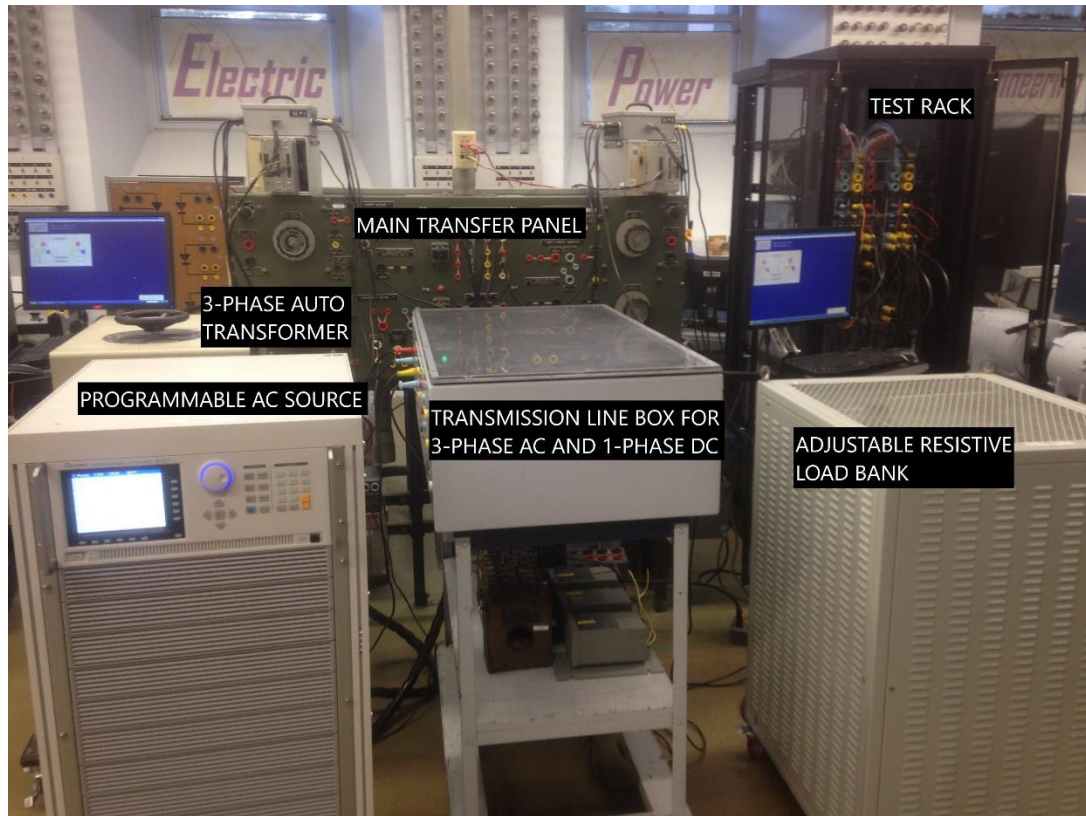
Figure 2.5 Layout of the Experimental AC/DC Microgrid Testbed in CEPE

The Chroma source has the capability to operate in a variety of settings even though they are not fully explored for the scope of this thesis. The local interface on the source, as seen in Figure 2.6, allows the user to set the type of voltage being generated as well as the magnitude and phase along with a range of other functions. Acting as the fixed AC power source at Bus1, the settings used for this setup are visible on the screen in Figure 2.6.
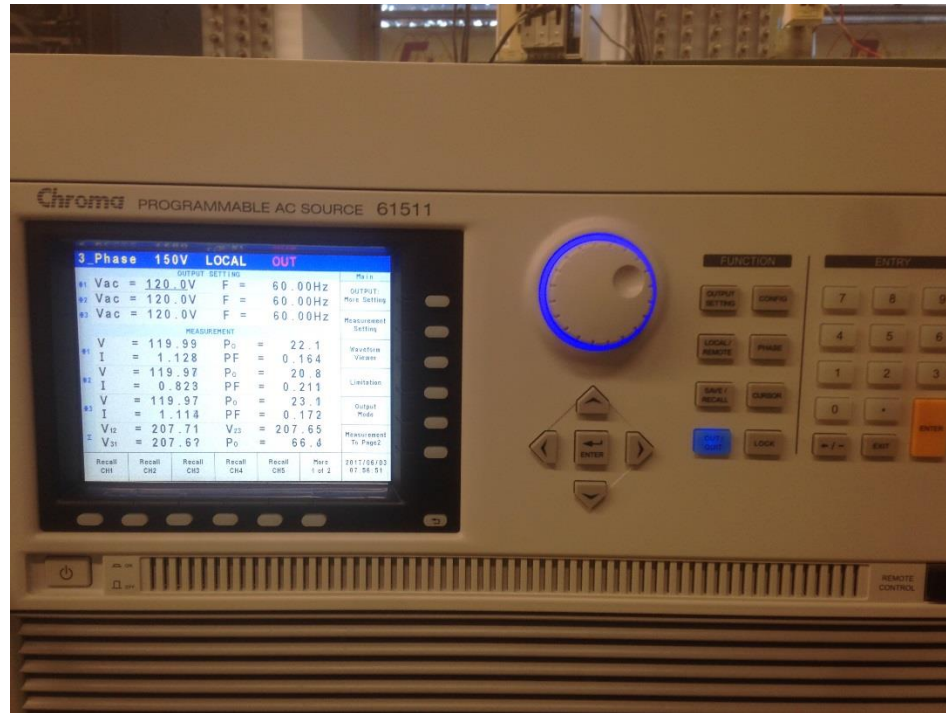
Figure 2.6 A Snap of the Chroma Programmable Source Acting as a 208 V$_{\text{LL}}$ Power Supply

In Figure 2.7, the Yokogawa power analyzer is on top followed by the three Chroma programmable loads. Loads 1 and 2 (top and middle) are connected to Bus 3, and Load 3 (bottom) is connected to Bus 4. Each of the loads are operating in a different mode which can be set either through their local interface on the load itself (the display screen) or remotely via the remote control interface pictured to the right of the loads in Figure 2.7. This interface is running on a Windows computer and is developed on a National Instruments LabVIEW platform. The development of the interface is discussed in detail in Chapter 3.
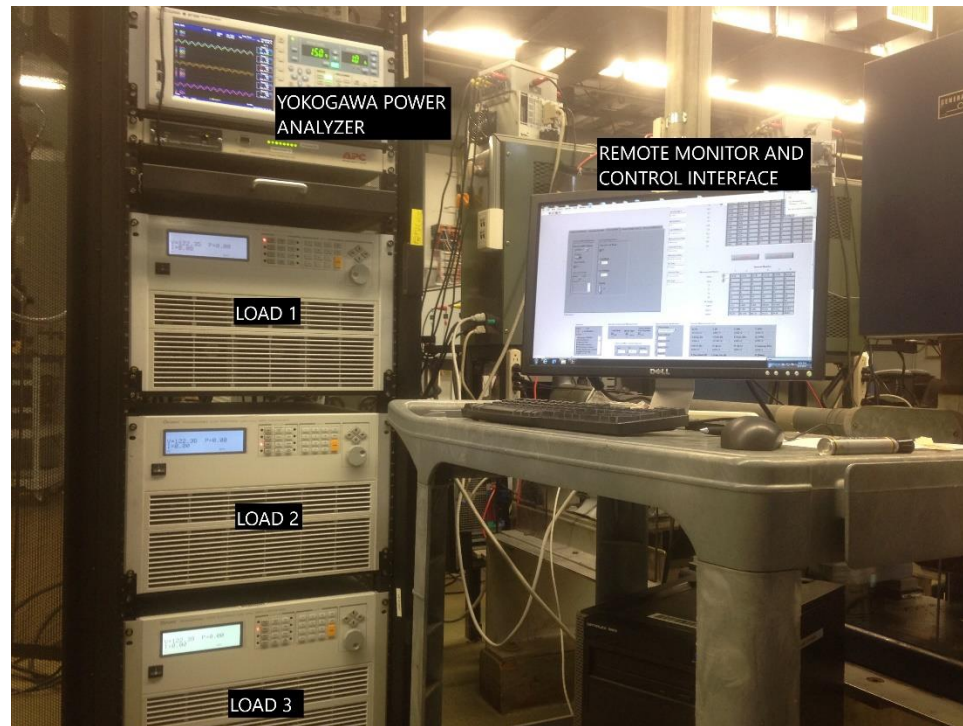
Figure 2.7 The Chroma Programmable Loads and Yokogawa Power Analyzer Side-by-Side With Their Remote Control Interface

The remote interface shows the measurements of the load along with its settings. The reliability of the remote measurements is verified through the waveforms captured on the Yokogawa power analyzer in real time. As discussed in Chapter 3, it is important for the monitoring capacity of the remote control interface to be reliable before it can take control actions based on those measurements.

The Chroma loads and the power analyzer are stacked in a test rack that was built for the purpose of having smarter loads and monitoring in the Drexel power laboratory. The rear of each test rack has connectors terminated at the loads, power analyzer and any other monitoring equipment. For this thesis, the building of a four bus AC and DC

microgrid meant that the wiring was intensive as can be seen in Figure 2.8. The connections

to the loads are insulated and color coded as shown to make wiring safe and easy.
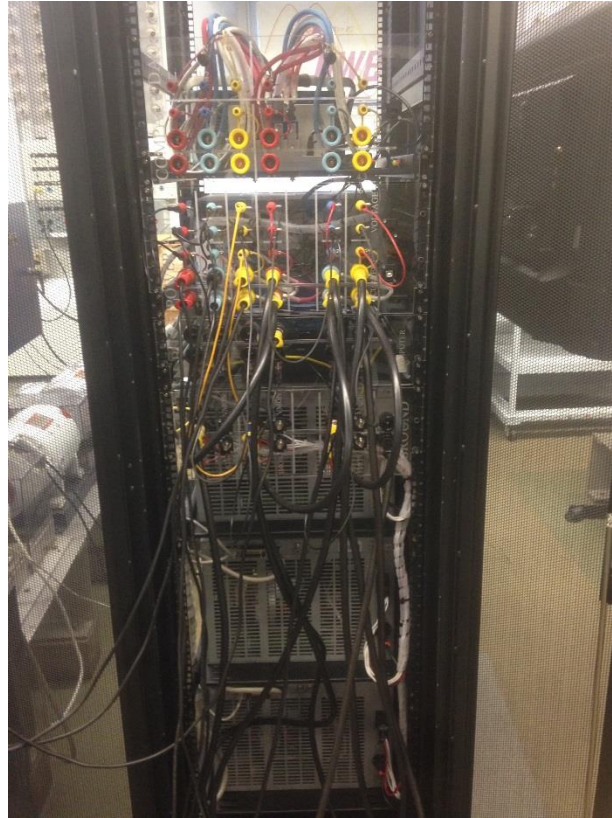
Figure 2.8 Rear Side of the Chroma Programmable Loads Showing Wiring

2.4. COMPONENTS USED

The components and equipment used in the experimental AC/DC microgrid testbed

setup are:

- 208 V_{LL} PECO 3 Phase AC source – This is the main power supply which is

  used to power the Chroma programmable source.

- Chroma Programmable source 61511 – The source is programmed to be a fixed, positive sequence three phase AC power supply of $208V_{LL}$ but it can also be programmed to emulate different distributed energy resources – a property that is not examined for the scope of this thesis.

- Visible disconnect switch – This is used to physically disconnect the main source of power from the rest of the circuit for safety purposes.

- Three phase autotransformer – While the source remains fixed, we adjust the autotransformer in order to obtain the desired voltage level at the DC bus.

- Signal conditioning box – This is present at both ends of the AC transmission line to measure the voltage and the current phasors.

- Remote Terminal Unit – The RTUs are the monitoring stations running a three-phase power transmission software that continuously displays the current and voltage levels.

- Diode Rectifier – The full wave diode rectifier converts the AC voltage into DC and is assumed to give

$$V_{dc} = \frac{3\sqrt{2}}{\pi} V_{LL} \qquad (2\text{-}1)$$

where,

  V_{DC}: Magnitude of voltage on the DC side of the rectifier at Bus 3

  V_{LL}: The input line-line voltage on the AC side of the rectifier at Bus 2

- Electrolytic capacitor – A Cornell Dubilier 1800uF capacitor is used to reduce the ripples in the DC signal obtained at the output of the rectifier.

- Chroma Programmable Load 63803 – These are programmable electronic loads that can operate in both AC and DC mode and in a variety of linear and nonlinear load models. They are discussed in detail in Chapter 3.

- Adjustable Resistive Load Bank – This is a DC variable resistor with a rating of 0.1-50A and 200VDC. It is used as a lumped parameter in the DC transmission line.

- Cables

  o 50A – 50A

    ▪ Connection between the 208V_{LL} power supply from PECO to the programmable Chroma source

    ▪ Connection between the programmable source and the visible disconnect switch

    ▪ Connection between the visible disconnect switch and the autotransformer

    ▪ Connections from the DC bus to the Chroma loads

  o 50A – 25A

    ▪ Connection between the autotransformer and the signal conditioning box (sending end)

  o 25A – 25A

    ▪ Connections between the signal conditioning boxes and the transmission line box

    ▪ Connection between the signal condition box (receiving end) and the Diode Rectifier panel

2.5. REAL LIFE REPRESENTATION OF LOADS

In real life, this represents an AC/DC microgrid with DC loads using rectified voltages. These type of microgrids are envisioned to have multiple bus connections/loads such as an Electric Vehicle charging station or an energy storage system in its recharging state connected to each of the DC buses. A major advantage of having a DC voltage serving a system that mainly operates loads in DC mode is that it reduces the need for power electronic converters that introduce harmonics and affect the stability of the system. Different loads in a DC grid have different characteristics. Electric heaters are a type of constant impedance (Z) loads; while a battery that is being charged draws a constant current (I) at all times. Loads that are connected through power electronic devices represent a constant power (P) load. The use of a programmable load in the laboratory allows the emulation of each of these loading scenarios during the course of the tests conducted in this thesis. This enhances the study of operating conditions as well as static stability issues beforehand.

The load remote monitoring and control computer signifies a smart meter which can continuously monitor the voltage, current and power values of the loads connected to it. The load characteristics are determined from these measurements which will be discussed further in Chapter 4. The load interface is also designed to be able to actuate the loads as and when necessary in order to achieve a suitable operating point.

3. TESTBED INSTRUMENTATION AND MEASUREMENT SYSTEM

3.1. OVERVIEW

For the successful implementation of any microgrid, the monitoring and communication systems play a very important role. Since the major strength of any microgrid is resilience and its ability to act as backup to a traditional power system, it must be able to sense and mitigate contingencies before they destabilize the network. For the testbed developed in this thesis, the control algorithm discussed in Chapter 4 relies on high quality system measurements, and so the measurement system plays a vital role.

For this purpose, each AC and DC bus is physically connected to a real-time monitoring system such that its state and readings can be observed at any point in time. This is made possible due to the smaller size of the network leading to a viable number of nodes accessible for metering. In microgrids where every node is not metered, estimation techniques are used to get a complete picture of the system under scrutiny. It is imperative that a microgrid testbed be observable at all times in order to implement any form of control features. This chapter outlines the instrumentation used for the development of the testbed and its measurement system.

The measurement and monitoring devices are divided into the AC side measurement and the DC side measurement. On the AC side of the microgrid, Data Acquisition cards are used to measure voltage and current phasors on either end of the transmission line. Signal conditioning boards are used to scale down the magnitudes of the

values and obtain a higher resolution for the readings. These complex measurements are then sent to the remote terminal units running an in-house power system software. In Figure 3.1 and Figure 3.2, screenshots of the AC power measurement software show how the AC side of the microgrid is being monitored. This measurement system was developed in house at Drexel CEPE to run Interconnected Power System Laboratory experiments [1,2]. The complex voltage and currents on each phase, along with the three-phase real and reactive powers, can be continuously monitored.
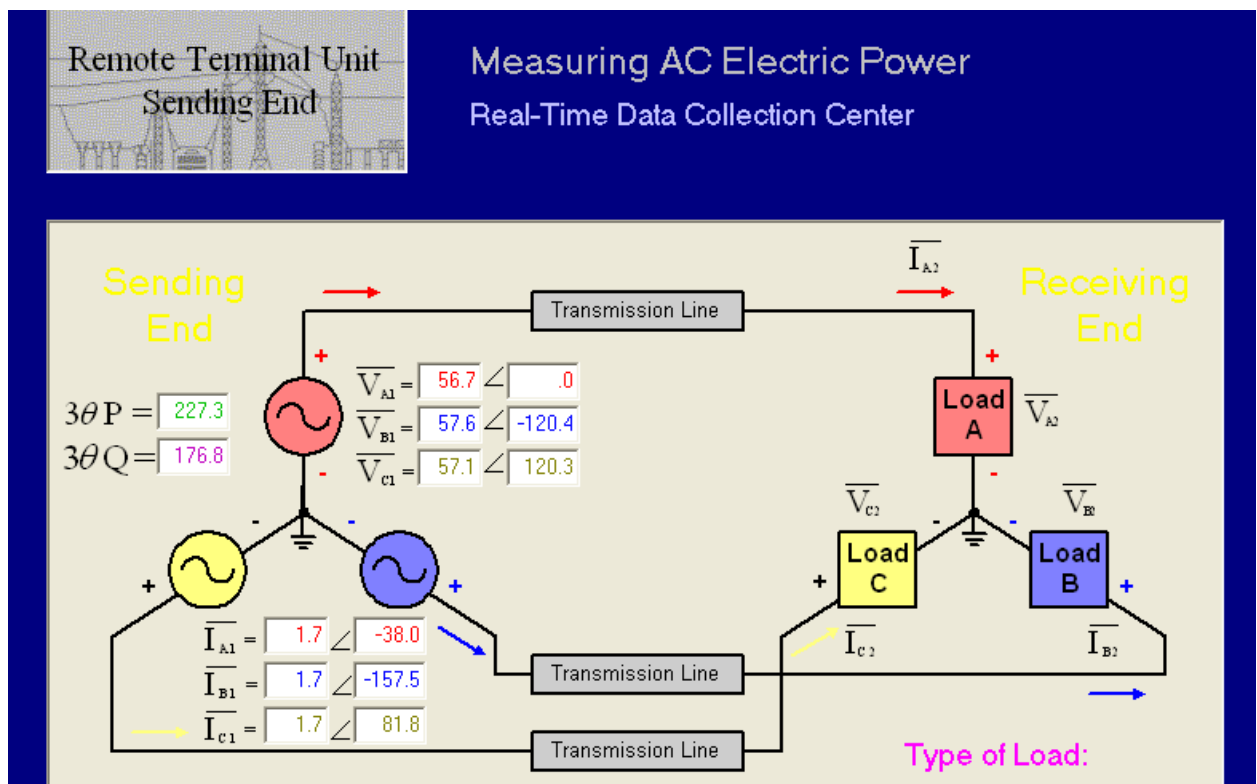
Figure 3.1 AC Side Measurements as Seen From the Sending End of the Transmission Line
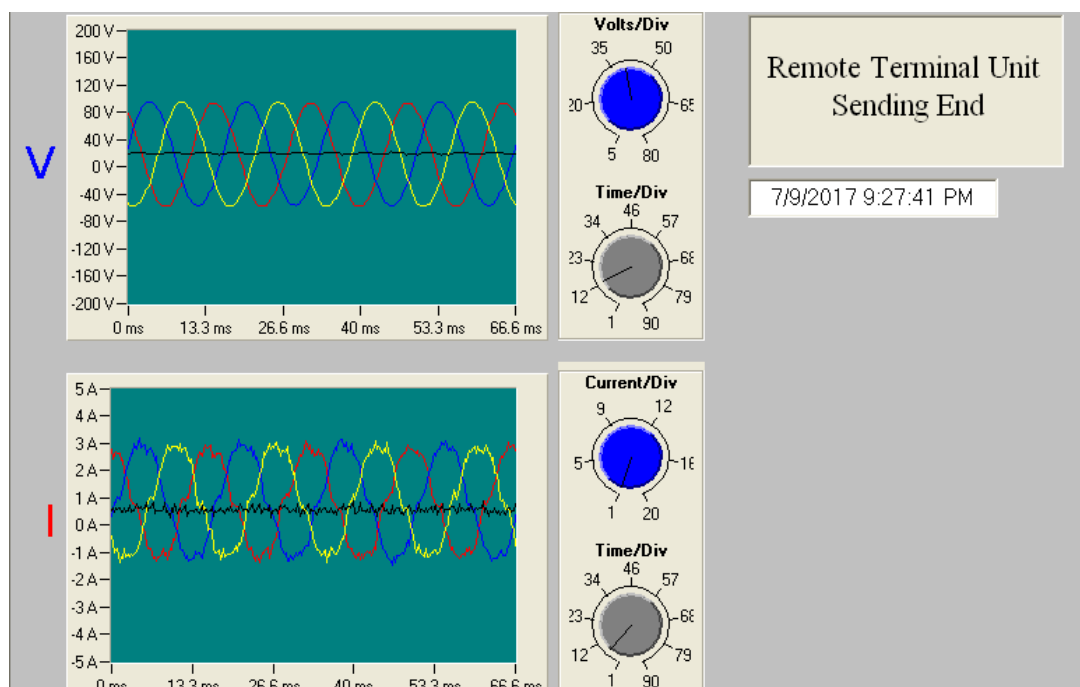
Figure 3.2 The Voltage and Current Waveforms at the Sending End of the Transmission Line

On the DC side, in order to monitor and actuate the three programmable loads simultaneously, a common platform was needed. LabVIEW provided this capability of remote monitoring and control by interconnecting with the loads through a IEEE 488 interface bus, commonly called GPIB (General Purpose Interface Bus). Assigning each Chroma unit a unique GPIB address allowed independent control and actuation of the loading types and parameters. The Yokogawa power analyzer is also remote monitoring enabled and is included in the LabVIEW software for ease of data collection. The three Chroma loads and the Yokogawa scope are daisy chained through GPIB cables and connected to the remote interface computer. This chapter details some of the theory behind the programmable loads and also, the design and operation of the LabVIEW interface.

3.2. CHROMA PROGRAMMABLE LOADS

In this thesis, Chroma 63803 AC/DC programmable electronic loads are used to conduct controllable loading experiments in a microgrid. These loads have a power rating of 3600W and can work with voltages between 50 and 350 V DC and currents between 0 and 36 A. These loads can simulate a wide range of AC/DC loading conditions for testing and experimental purposes as shown in Figure 3.3. They are designed to test Uninterrupted Power Supply, off-grid inverters, AC sources and power devices like switches, circuit breakers and fuses.
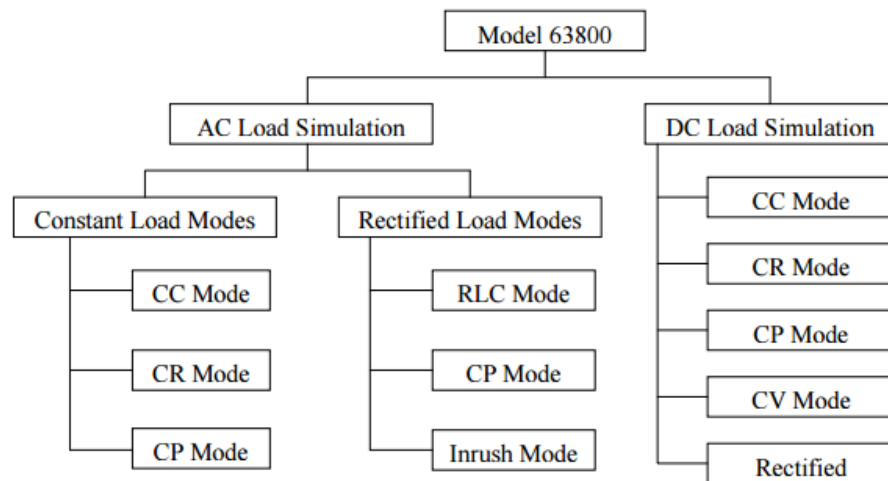
Figure 3.3 Load Simulation Types on Chroma 63803

The loads in the experimental testbed can be operated as any of the DC load simulation modes from Figure 3.3. For the control methodology implemented in this thesis, they are operated as a static load in one of the constant load modes. These load modes are as follows

    i.   Constant Current Mode (Fig 3.4(a)):

- The load sinks a constant value of current regardless of the input voltage

- The slew rate determines the rate of change of input current from one level to another

ii. Constant Resistance Mode (Fig 3.4(b)):

- The load sinks a current linearly proportional to input voltage according to programmed resistance

- Power source impedance has to be low enough to prevent fluctuation in current from voltage variation

iii. Constant Power Mode (Fig 3.4(d)):

- The load draws a constant power from the source irrespective of the bus voltage

- Load current depends on non-linear $P = V*I$
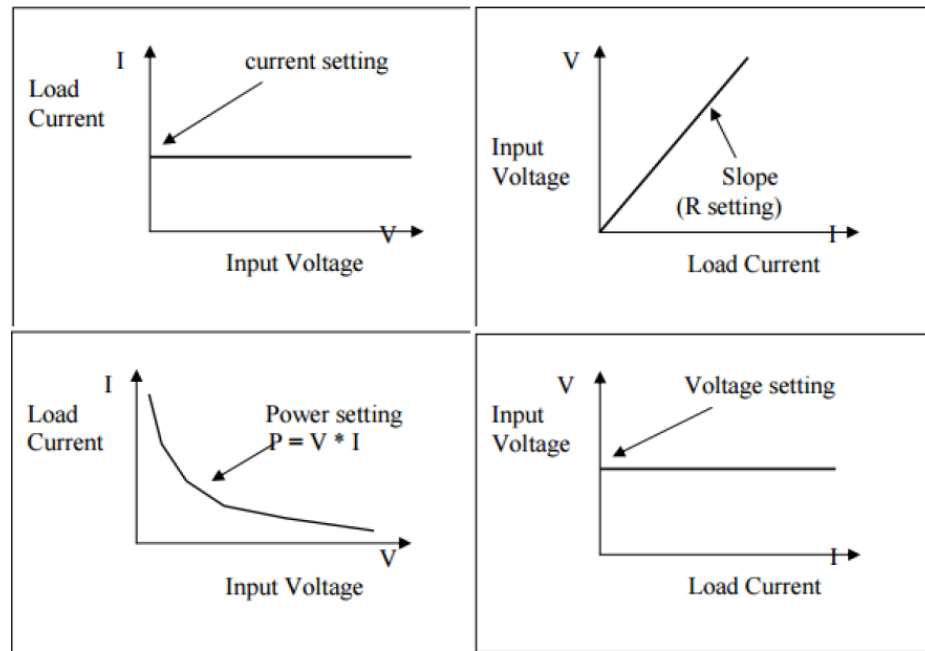
Figure 3.4 Different Load Type Characteristics (Clockwise From Top Left) (a) Constant Current (b) Constant Impedance (c) Constant Voltage (d) Constant Power

3.3. DEVELOPMENT OF THE INTERFACE

LabVIEW was chosen as a platform because of its data acquisition and handling capabilities. LabVIEW has a graphical system design approach that allows for the use of the same tools and platforms both in the research/development phase in an academic setting as well as deployment phase. This graphical system provides an easy and effortless integration with the latest technology such as the devices used in this research. Moreover, the makers of the equipment used in this research also intended for the remote operation of the devices to be done over LabVIEW by providing the buyers with LabVIEW interfacing drivers. The testbed devices employed on the DC side like the loads and the scope have a serial communication port (GPIB, RS232 etc.) which can be used to digitally connect to LabVIEW.

For the purpose of this research, each of the loads as well as the power analyzer are controlled independently by using a different GPIB address for each of them. Figure 3.5 below shows a screenshot of the initialization window for the Chroma loads and Yokogawa scope used in the microgrid testbed. Each of the devices connected to the remote interface can be initialized and controlled independent of each other. In the initialization window of a Chroma load as shown in Figure 3.5, the GPIB address as well as the operating modes of the load are set. The operating modes can also be changed during the run time of the experiment. If any errors occur during the execution of the software for the remote control of the testbed devices, a corresponding error code and message appears in the window below the initialization of the device as seen in Figure 3.5.
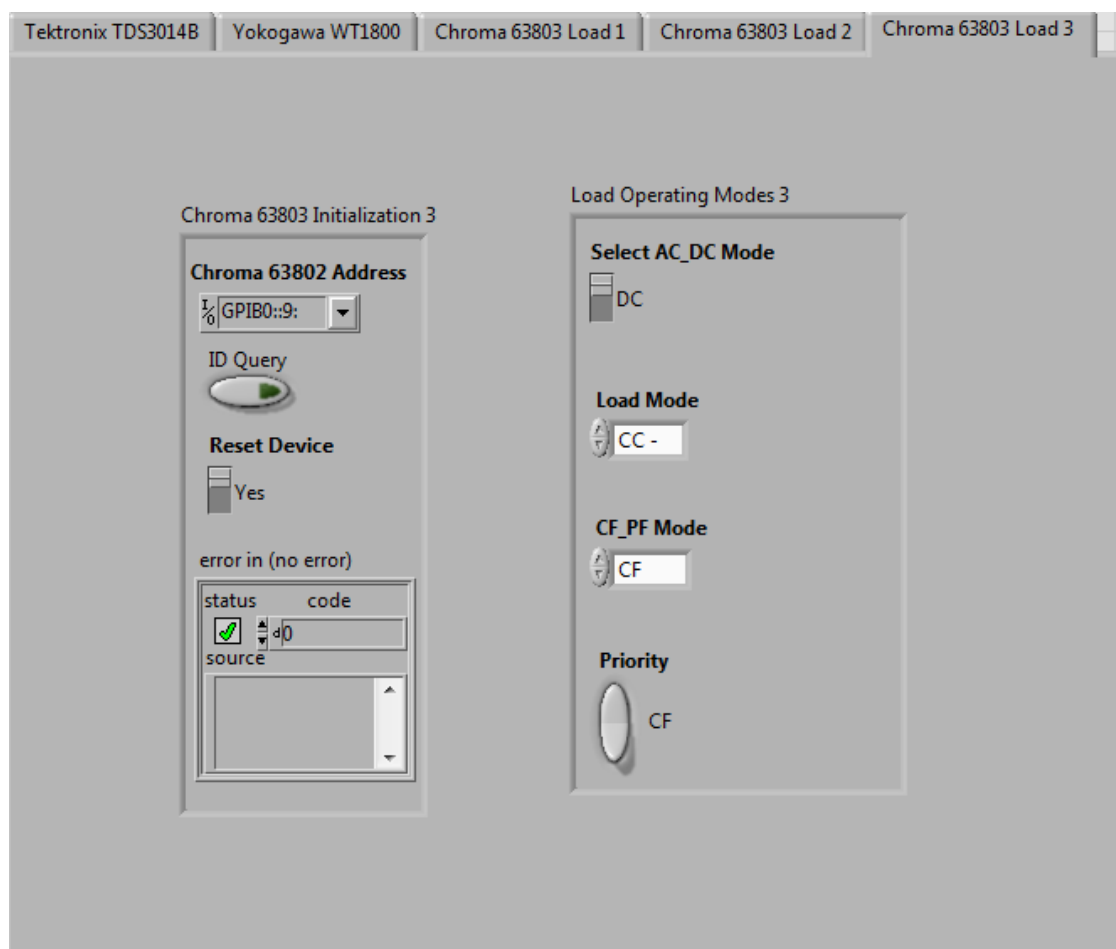
Figure 3.5 Setting GPIB Address and Load Modes for the Chroma Programmable Load

Once the loads and the scope have been initialized, the load parameters are set. Each of the loads are independently controlled and the parameter window is programmed to display only the necessary windows depending on the corresponding load mode. In Figure 3.6, an example of setting constant current load parameters is shown. The current value and the maximum load current values are set. The I_P (max) setting is to ensure that the current drawn by the programmed load does not exceed the current rating of the Chroma load, as well as other upstream circuit components, at any time. Here, the crest factor was

set to resemble a pure sinusoidal wave and a unity power factor indicating a resistive load type. These can also be changed to simulate different load types. Once the settings have been confirmed, the load is triggered by toggling the load state to ON. In case of any errors, such as exceeding the power handling capacity, the load will trip instantly and the respective error message is displayed in the initialization window.

Figure 3.6 Assigning Load Parameters to the Load and Toggling the Load State

The load characteristics of all three programmable loads in the system are measured simultaneously and displayed. Figure 3.7 shows a snapshot of the measurements obtained when the microgrid is running in the four bus AC/DC mode. Load 1 is connected to Bus 4 and is seen to have a lower bus voltage than Loads 2 and 3 which are connected to Bus 3.

The measurements received from the load are then verified by checking against the voltage and current waveform values on the calibrated Yokogawa scope. Also, each of the loads are operating in different modes. The measurements can be exported to Microsoft Excel at any time for analysis.

V, [V]	I, [A]	P, [W]	S, [VA]
69.18E+0	1.00E+0	67.07E+0	0.00E+0
V_Peak, [V]	**I_Peak, [A]**	**P_Peak, [W]**	**Q, [VAR]**
0.00E+0	228.63E+0	0.00E+0	0.00E+0
THD_V, [%]	**CF, [p.u.]**	**PF, [p.u.]**	**Frequency, [Hz]**
0.00E+0	0.00E+0	0.00E+0	0.00E+0
V_Overshoot, [V]	**I_Peak_Pos, [A]**		**R, [Ohm]**
228.63E+0	228.63E+0		0.00E+0
V_Undershoot, [V]	**I_Peak_Neg, [A]**	**Time Stamp**	
500.00E+0	500.00E+0	8:10:17.685 PM 6/2/2017	

Chroma Measurements Out 2

V, [V]	I, [A]	P, [W]	S, [VA]
74.89E+0	2.00E+0	149.86E+0	0.00E+0
V_Peak, [V]	**I_Peak, [A]**	**P_Peak, [W]**	**Q, [VAR]**
0.00E+0	104.26E+0	0.00E+0	0.00E+0
THD_V, [%]	**CF, [p.u.]**	**PF, [p.u.]**	**Frequency, [Hz]**
0.00E+0	0.00E+0	0.00E+0	0.00E+0
V_Overshoot, [V]	**I_Peak_Pos, [A]**		**R, [Ohm]**
104.26E+0	104.26E+0		0.00E+0
V_Undershoot, [V]	**I_Peak_Neg, [A]**	**Time Stamp**	
73.88E+0	73.88E+0	8:10:17.805 PM 6/2/2017	

Chroma Measurements Out 3

V, [V]	I, [A]	P, [W]	S, [VA]
74.96E+0	500.00E-3	37.52E+0	0.00E+0
V_Peak, [V]	**I_Peak, [A]**	**P_Peak, [W]**	**Q, [VAR]**
0.00E+0	85.99E+0	0.00E+0	0.00E+0
THD_V, [%]	**CF, [p.u.]**	**PF, [p.u.]**	**Frequency, [Hz]**
0.00E+0	0.00E+0	0.00E+0	0.00E+0
V_Overshoot, [V]	**I_Peak_Pos, [A]**		**R, [Ohm]**
85.99E+0	85.99E+0		149.92E+0
V_Undershoot, [V]	**I_Peak_Neg, [A]**	**Time Stamp**	
74.01E+0	74.01E+0	8:10:17.549 PM 6/2/2017	

Figure 3.7 Monitoring the Load Measurements Simultaneously

Achieving real time simultaneous measurements of the DC side loads builds the foundation to implement load control on the DC side of the microgrid. The Yokogawa power analyzer is calibrated for accurate voltage and current measurements and is used as a reference. The Chroma loads are continuously monitored and the measurements obtained are verified on the Yokogawa scope. Once the validity of the measurements has been established, control of the load is possible by taking the measurements obtained to be accurate values. In Chapter 4, the control algorithms discussed rely on the measurements in order to build a linear approximation of the load characteristics. Thus, the instrumentation and measurement system plays an important role in the microgrid testbed developed.

4. SENSITIVITY BASED VOLTAGE CONTROL VIA MEASUREMENTS

4.1. OVERVIEW

The Power-Voltage "P-V" curve has been widely used to analyze power system behavior under varying loading conditions [15]. Several stability studies have been conducted on both AC microgrids [16,17] and DC microgrids [18]. The causes of stability issues are varied ranging from the type of operation (islanded or grid-connected) to the presence of power electronic interfaces. This thesis looks at microgrid loading issues, with a focus on undervoltage regulation in particular, present in the DC buses of the microgrid.

The knee of the characteristically non-linear P-V curve is the limit that indicates the maximum loading point, beyond which the voltage collapses with slight perturbations in the system. Since voltage instability is a local phenomenon that can have widespread effects, a collapse in voltage at any of the buses in the microgrid can lead to complete voltage collapse of all microgrid buses. Hence it is essential to have a control methodology for voltage regulation to implement a successful microgrid.

In the microgrid testbed presented in Chapter 2, a drop in the DC bus voltage below a threshold value is considered an overloading condition. This thesis uses a linear sensitivity approach to determine the near continuous control settings (with a precision of 10^{-2} actual units) of loads to regulate the voltage of the bus under consideration. The difference between actual operating point voltage and the desired threshold voltage is what the control strategy aims to reduce through load shedding. The continuously variable

programmable loads allow shedding the required amount of power as opposed to other hardware loads that can only reduce power consumption in discrete steps. In this thesis, the programmable source is kept constant; therefore, generation control techniques are beyond the scope of this thesis. The proposed load control algorithm calculates the amount of load to be shed by each load.

When multiple loads are present on the same bus, the controller can demand any one load to shed the entire amount required to raise the voltage level, or each of the loads can be targeted individually depending on their participation factors, as described in Section 4.2. The success and effectiveness of the different control approaches discussed in Section 4.2 presents an interesting insight into DC loads in a hybrid microgrid that can be useful to many microgrid controller developers.

This chapter discusses the load control approaches used to achieve load shedding in a microgrid. Specifically, it presents:

- In Section 4.2, the formulation of a load shedding problem and proposed load control algorithm;

- In Section 4.3, the experimental results of the proposed control strategy on a three bus microgrid system and comparison;

- In Section 4.4, the experimental results of the proposed control strategy on a four bus microgrid system.

4.2. PROBLEM FORMULATION AND CONTROL METHODOLOGY

Traditionally in power distribution systems, load shedding has been done in a rudimentary manner where the customers connected to a bus that experiences a heavy loading condition are requested to reduce their power consumption by ΔP. This approach does not consider the type of load being shed – only the initial and final power being used by the load to increase the voltage on a bus by ΔV. While in larger systems this load shedding control signal is realized without major problems, in a small microgrid system it is imperative to have a more insightful approach to how much load the individual loads shed. The problem in this thesis focuses on DC portion of the microgrid. The DC voltage at the bus is assumed to change monotonically with load change, such that reaching a threshold voltage will require just a minimal amount of load change.

A load shedding method is determined that brings the voltage at an undervoltage bus to a pre-determined threshold voltage value. The research done in this thesis focuses on the DC grid with three loads connected to the DC bus facing an overloading condition and a bus voltage of V_K. The objective is to implement a control algorithm that raises the bus voltage to the threshold voltage V_{TH} within measurement tolerance. There may be many non-unique solutions to achieving the objective of attaining the threshold voltage within an acceptable tolerance i.e. $|V_{TH} - V_K| < \varepsilon$ and a power metric is used to analyze the efficiency of each solution. The power metric compares the change in average power consumption P_{DC} of each load that is actuated to achieve the solution. The power being drawn by the load is calculated as a function of the nominal value of its load type:

i.   For constant power loads,

$$P_{DC} = P_{nom} \qquad (4\text{-}1)$$

ii.   For constant current loads,

$$P_{DC} = I_{nom} * V_K \qquad (4\text{-}2)$$

iii.   For constant impedance loads,

$$P_{DC} = \frac{V_K^2}{R_{nom}} \qquad (4\text{-}3)$$

where,

P_{DC} is the average DC power consumed by the load

P_{nom} is the nominal power of the constant power load

I_{nom} is the nominal current of the constant current load

R_{nom} is the nominal resistance of the constant impedance load

V_K is the voltage at the bus where load shedding is done

A load shedding problem for the testbed described in Chapter 2 is formulated as follows:

Given: The voltage $\Delta V = V_{TH} - V_K$ to be recovered at bus K to reach the threshold voltage level, along with the voltage sensitivities to get new load settings, determine a load shedding algorithm such that

$$|V_{TH} - V_K'| < \varepsilon \qquad (4\text{-}4)$$

where,

V_{TH} is the desired threshold voltage

V_K' is the bus voltage after implementing load control

ε is the allowable difference due to noise in measurements

Since many non-unique paths are available, the power metric used to compare the multiple solutions that bring the bus voltage to V_{TH}, where X, Y and Z represent the average power P_{DC} being consumed by each of the three loads respectively on the bus:

$$\Delta P = \frac{\cdot\sqrt{(X_0-X_1)^2+(Y_0-Y_1)^2+(Z_0-Z_1)^2}}{\cdot\sqrt{X_0{}^2+Y_0{}^2+Z_0{}^2}} \qquad (4\text{-}5)$$

where,

X_0, Y_0, Z_0 are the initial power consumption of the loads

X_1, Y_1, Z_1 are the final power consumption of the loads

The power metric computes the average percentage change in power consumed by each load which directly relates to the path travelled by the operating point. While it is possible to limit the power consumption of each load, between an upper and lower constraint as shown below, it is not considered during the load shedding operations done in this thesis.

$$X > X_{min}, Y > Y_{min}, Z > Z_{min}; \qquad (4\text{-}6)$$

$$X < X_{max}, Y < Y_{max}, Z < Z_{max} \qquad (4\text{-}7)$$

The target of the load shedding in this case is defined as reaching the threshold voltage V_{TH} such that $|V_{TH} - V_K'| < \varepsilon$. For qualitative comparison of different load control strategies that attain a solution, their power metrics were calculated. Thus, it is possible to identify the load shedding approach that causes the least disruption of nominal service to the loads connected to the bus where load shedding occurs.

While it is possible to find the solution to the formulated load shedding problem in many ways, this thesis proposes a sensitivity based control algorithm for individual vs aggregate loads and different load modes. This proposed load control algorithm for the three DC load problem formulated above is described in Section 4.2.1 and other more traditional control strategies are outlaid in Section 4.2.2. The results of testing these control algorithms are presented in Section 4.3.

4.2.1. PROPOSED CONTROL ALGORITHM

Given the number and type of programmable loads, the proposed algorithm consists of five main steps:

Step 1. Identification of operating point V_K of the overloaded bus via measurements

Step 2. Determining the voltage sensitivity and participation factor of each loads

Step 3. Calculating an estimated amount of power to be shed by each load and translating that to its respective load type

Step 4. Actuate the control and check if $|V_{TH} - V_K'| < \varepsilon$. If YES, proceed to Step 5, or else go back to Step 1 and update the operating point of the load to V_K'

Step 5. Calculate the power metric of the obtained solution to compare its competitiveness to other alternate solutions

Detailed steps are described below.

Step 1. Identification of operating point and load properties

For experimental purposes, the three loads connected to the DC bus are operated in constant power, constant impedance and constant current mode respectively so as to represent a ZIP load on the bus. It is assumed that each of the loads has an average initial value at which it operates during the overloading condition of the bus. The load mode and its value is set on the control center as described in Figure 3.6.

By varying the load around this initial value, we can plot its P-V curve. For example, in order to find the P-V curve of the constant power load, only the constant P load varies, while the constant current and constant impedance loads are kept, indeed, "constant". The operating voltage of the bus V_K is noted from the central measurement center and the difference from the threshold voltage, which is the amount of voltage the load shedding algorithm aims to make up, is calculated as

$$\Delta V = V_{TH} - V_K \qquad (4\text{-}8)$$

Step 2. Determining voltage sensitivity and participation factor of each load

The measurement based $\frac{dV}{dP}$ sensitivity is obtained for each load by a linear approximation of its P-V curve. The curves are plotted for each load by varying them individually around the operating point V_K of the bus with the loads at their

initial settings. Different results may be obtained by calculating voltage sensitivities at different voltage levels, but that aspect is not discussed in this thesis. Also, in order to get sensitivity based participation factors, the proportion of the voltage sensitivity of each load with respect to each other is calculated.

$$\alpha_i = \left. \frac{\frac{dV}{dP_i}}{\frac{dV}{dP_1} + \frac{dV}{dP_2} + \cdots + \frac{dV}{dP_N}} \right|_{V = V_K} \qquad (4\text{-}9)$$

$$i = 1, 2, \ldots \ldots N$$

where,

    in this work, $N = 3$

    $\frac{dV}{dP_1}, \frac{dV}{dP_2}, \frac{dV}{dP_3}$ are the individual voltage sensitivities

    $\alpha_1, \alpha_2, \alpha_3$ are the participation factors of the loads

Step 3. Calculation of estimated load amount to be shed by each load

The participation factors decide the contribution of each load to the overall load shedding on the bus. The load that has a higher participation factor brings about a larger change in the bus voltage and hence reduces its demand by a larger proportion as compared to the rest of the loads. This is akin to capacity based participation factors used in distributed slack bus modelling in [20], where the contribution of different distributed resources is based on their individual participation factors.

Step 3.1. Calculate *ΔP* target for each load

First, the total amount of power to be shed in order to make up the voltage difference to the threshold voltage is calculated from ΔV and the voltage sensitivity of the loads. This value is calculated for each of the loads and would be amount of power the respective load shed if it were the only load participating in load shedding:

$$\Delta P_i^T = \frac{\Delta V}{\frac{dV}{dPi}} \qquad (4\text{-}10)$$

$$i = 1, 2, \dots \dots N$$

where,

in this case $N = 3$

ΔV is the amount of voltage to be recovered

ΔP_i^T is the total amount of power to be shed by load i to recover ΔV

$\frac{dV}{dPi}$ is the voltage sensitivity of the load i

Then, the contribution of each load to the overall load shedding at the bus is calculated by multiplying each ΔP_i^T by their participation factors. Amount of power shed by each load:

$$\Delta P_i = \alpha_i * \Delta P_i^T \qquad (4\text{-}11)$$

$$i = 1, 2, \dots \dots N$$

where,

in this case $N = 3$

α_i is the participation factor of load i

ΔP_i is the amount of power shed by load i in proportion

with other loads on the bus

Step 3.2. Calculate equivalent load setting for each load

The amount of power to be shed is then translated to an equivalent

load shed amount in terms of the parameter of the particular load mode that

each load is in, and the corresponding load setting is calculated.

I. Constant Current Load model having an initial operating current I_{nom}:

$$P_{orig} = V_K * I_{nom} \qquad (4\text{-}12)$$

$$P_{new} = P_{orig} - \Delta P_i \qquad (4\text{-}13)$$

$$I_{new} = \frac{P_{new}}{V_{TH}} \qquad (4\text{-}14)$$

II. Constant Power Load model having an initial operating power P_{nom}

$$P_{new} = P_{nom} - \Delta P_i \qquad (4\text{-}15)$$

III. Constant Impedance Load model having an initial operating resistance

R_{nom}

$$P_{orig} = \frac{V_K^2}{R_{nom}} \qquad (4\text{-}16)$$

$$P_{new} = P_{orig} - \Delta P_i \qquad (4\text{-}17)$$

$$R_{new} = \frac{V_{TH}^2}{P_{new}} \qquad (4\text{-}18)$$

where,

$I_{nom}, P_{nom}, R_{nom}$ are the original load parameters of the load

$I_{new}, P_{new}, R_{new}$ are the new load parameters the loads are

actuated to by the control center

P_{orig} and P_{new} are the powers consumed by the loads before and after actuation respectively

Step 4. Checking the results of the load shedding and determining success

Once the load setting has been calculated, the load is actuated to the new value at the control center, and the new bus voltage is observed to quantify success of the operation. For a 120 V_{DC} bus, a small error percentage of about 1.67% or $\varepsilon < 2V$ is permissible to account for noise in the instrumentation system. Then, the difference of the new bus voltage V_K' from the desired threshold voltage is calculated and:

i. If $|V_{TH} - V_K'| < \varepsilon$

The load shedding problem has been satisfied and PROCEED to Step 5.

ii. If $|V_{TH} - V_K'| > \varepsilon$

Update the operating bus voltage V_K as V_K' in equation (4-8) to calculate new ΔV and GO TO Step 3.

Step 5. Determining the competitiveness of the successful control algorithm

Once a successful control solution has been obtained, its relative "efficiency" to other successful control solutions, discussed in the following subsection, is calculated using the power metric described in the problem statement.

Hence, the load shedding algorithm proposed by this thesis incorporates the ZIP load model types as well their participation factors. In order to comprehend its solution quality, some other methods to the load shedding problem are presented in the following section. Once different solutions have been obtained, the "efficiency" of each solution is examined through the power metric. It is referred to as efficiency since it gives an indication of the quality of the control algorithm that obtains the desired result by minimizing the percentage change in operating powers of the loads, thereby minimizing disruption in service to the loads.

4.2.2. ALTERNATE CONTROL ALGORITHMS

In order to demonstrate the effectiveness of the proposed load control algorithm, this thesis performs experiments using two other scenarios of load control:

1. SCENARIO 1 – AGGREGATE LOAD SHEDDING

This load control scenario compares the proposed control algorithm with load shedding methods employed in larger power systems. In traditional power distribution systems, the loads are considered to be aggregates connected to each bus and their load modes are not always reflected in any load shedding analysis. In

these cases, the controller merely sheds the required amount of power from the customers connected to a grid without consideration of the load model type or the amount of power consumed by the loads being shed. The load shedding in this case is less effective because the power being consumed by the loads is not considered as a function of its load mode.

When the load model is not taken into account, an aggregate voltage sensitivity for the bus is used to determine the net power ΔP to be shed at the bus. This is assumed to be the average voltage sensitivity of the N loads connected to the bus:

$$\frac{dV}{dP} = \frac{\frac{dV}{dP1} + \frac{dV}{dP2} + \cdots + \frac{dV}{dPN}}{N} \qquad (4\text{-}19)$$

where,

in this case $N = 3$.

The amount of power ΔP to be shed to reach the threshold voltage by increasing the bus voltage by ΔV from equation (4-8) is then calculated as:

$$\Delta P = \frac{\Delta V}{\frac{dV}{dP}} \qquad (4\text{-}20)$$

The loads are viewed merely as sinks of power and an equal amount of power is shed from each load:

$$\Delta P_i = \frac{\Delta P}{N} \qquad (4\text{-}21)$$

The power being consumed by each load after shedding load is then calculated to be:

$$P_i^{new} = P_i^{nom} - \Delta P_i \qquad (4\text{-}22)$$

where,

$i = 1, 2, \ldots. N$

in this case $N = 3$

The bus voltage is observed after actuation of the loads and Step 4 from Section 4.2.1 is performed to check the success of the load shedding. Once a successful load shedding solution has been found, the power metric is calculated.

2. SCENARIO 2 – SOLO LOAD SHEDDING WITHOUT PARTICIPATION FACTOR

This scenario represents a case where a microgrid controller decides to target just one customer to rectify an overloading condition on the bus to reduce the number of customers who must participate in load shedding. Since there are three loads - each of a different load mode - in this microgrid testbed, three cases are considered under Scenario 2 where each of the loads are targeted individually for load shedding. The calculations are done for each case and the success of each case is examined. Here, the ZIP load types are considered, and the amount of load to be shed is calculated based on the load mode that each load is operating in. The individual voltage sensitivities are used to determine the total load shed by a singular load similar to equation (4-10) in the proposed load shedding control.

The corresponding parameter to be shed for different ZIP load types is calculated according to equation (4-12) through equation (4-18) in Step 3.2 of the

proposed algorithm, with the ΔP_i value replaced with ΔP_i^T calculated from equation (4-10). This type of load shedding is done on just one load at a time and the other loads on the bus operate at its original values. The success of load shedding for each case is again determined according to Step 4 from Section 4.2.1, and then its power metric is calculated.

The different control methodologies are compared against the proposed load control where each of the loads contribute to reducing power consumption on the bus by shedding an amount of load proportional to its voltage sensitivity. These scenarios are examined to demonstrate the importance of the participation factors and consideration of ZIP load types in solving the load shedding problem, and their impact on minimal service disruption quantified by having lower power metrics. Having a higher value of power metric for a solution indicates a larger drop in power delivered to the customers and is a less than ideal situation for a microgrid controller. So, it is not only important to perform load shedding that increases the voltage to a threshold value, this thesis argues that it is imperative to do it in such a way that the customers connected to a microgrid face least deviation from nominal operating points. This testbed illustrates very practical challenges in microgrid control and the proposed solution to the load shedding control problem, along with the alternate methods, is tested in Section 4.3.

4.3. RESULTS OF LOAD SHEDDING ON THE THREE BUS MICROGRID

The load shedding problem is tested on the 3 bus microgrid testbed. Three loads are connected to the 120V DC bus in Figure 2.2 each operating in a different static load model and arbitrarily assigned load setting values to mimic the several types of load in real world. These load types are set in the central control center.

For the experiment conducted in this thesis, the threshold voltage level is assumed to be 90V_{DC}, below which the DC bus is said to have a poor voltage profile. The threshold value can be chosen differently to run different tests. The load values are set such that at their initial values, the operating point of the bus is below the voltage threshold value.

Table 4.1 Initial Load Setting for the Load Shedding Problem on 3 Bus Microgrid

LOAD NUMBER	LOAD TYPE	INITIAL VALUE	BUS	COMPUTED POWER ($V_3 = 75.7$V)
1	Constant Current	1A	3	75.7W
2	Constant Power	150W	3	150W
3	Constant Impedance	150Ω	3	38.2W
TOTAL				263.9W

Now, the P-V curve of each individual load connected to Bus 3 is obtained by varying each load +/-10% from its average initial operating value while keeping the other

two loads constant at their initial values. After plotting the P-V curves, the voltage

sensitivity of each load is obtained with respect to power by a linear approximation of the

P-V curves. The P-V curves of the loads are obtained as shown in Figure 4.1 and the

calculated values of $\frac{dV}{dP}$ for each load are shown below it.
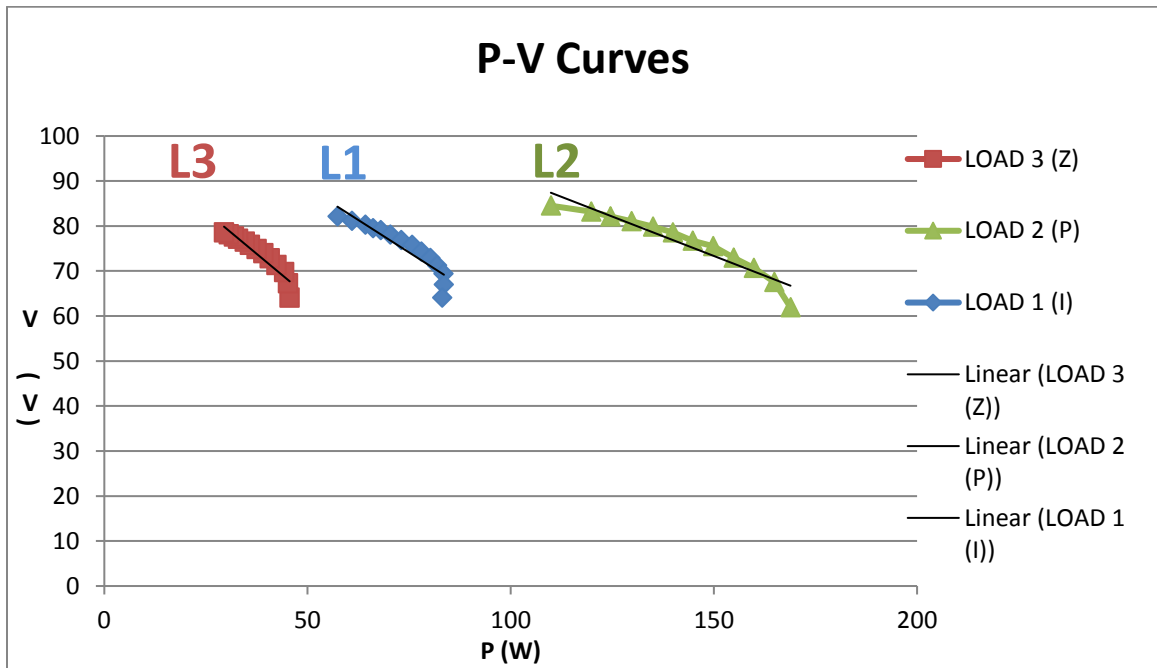
Figure 4.1 P-V Curves generated by Varying Each Load Connected to Bus 3 Individually (No Load V₃ = 120V)

$$\frac{dV}{dP1} = 0.577$$

$$\frac{dV}{dP2} = 0.35$$

$$\frac{dV}{dP3} = 0.752$$

In the case of an undervoltage condition, where the bus voltage goes below the threshold value, the controller aims to determine the best way to actuate the loads using a load shedding algorithm. When all the loads are operating at their initial values, the bus voltage operating point is at 75.7V. It is desired to increase the voltage at the bus to the threshold voltage 90V i.e. from equation (4-8), $\Delta V = 14.3V$.

Thus, the controller must determine how the programmable loads respond in shedding some load either individually, or in proportion with the other loads, to increase the bus voltage by ΔV. In order to analyze the varied success of the different load shedding approaches discussed in Section 4.2 against the backdrop of the load shedding problem formulated, the two metrics are compared:

    i. $|V_{TH} - V_K'|$ value

    ii.   Percentage change in average power drawn by each load

4.3.1. PROPOSED LOAD SHEDDING ALGORITHM

The extent of load shed by each load is decided by the ratio of their voltage sensitivities. From equation (4-9), we get the participation factors of each of the loads as:

$$\alpha 1 = 0.34$$

$$\alpha 2 = 0.21$$

$$\alpha 3 = 0.45$$

The total amount of load to be shed by each load is calculated according to equation (4-10), which is multiplied by its participation factors to get the proportional amount of load shed such as in equation (4-11). From these, we find that

$$\text{LOAD 1 has to shed } 0.34 * 24.78W = 8.43W$$

$$\text{LOAD 2 has to shed } 0.21 * 40.86W = 8.58W$$

$$\text{LOAD 3 has to shed } 0.45 * 19.01W = 8.55W$$

Since each of the loads are of a different load model, their equivalent load shed amount and therefore their final load setting is calculated using equations (4-12) through (4-18). Calculating these, LOAD 1 is changed to 0.75A, LOAD 2 is changed to 141.2W and LOAD 3 is changed to 273.23Ω.

At the end of this simultaneous actuation of all three loads - done at the control center - the bus voltage rises to 88.3V and the stopping criteria $|V_{TH} - V_K'| = 1.7V$. Since this is less than ε, the load shedding stops here according to Step 4 of the algorithm. The resulting power metric of the proposed load control strategy is calculated to be 8.5%. This value indicates relatively low disruption to the power supplied to each of the loads.

4.3.2. SCENARIO 1

For aggregate load shedding, the individual load models are not considered and the voltage sensitivity of the bus, calculated using equation (4-19) as the average of the three voltage sensitivities, is 0.56. With a bus voltage of 75.7V, the average power drawn by each load at its initial value is calculated and the total load delivered at the bus is found to be

$$P_{L1}\ (75.7V) +\ P_{L2}(150W) + P_{L3}\ (38.2W) = 263.9W$$

where P_{L1}, P_{L2} and P_{L3} are the average powers being consumed by LOAD 1, LOAD 2 and LOAD 3 respectively.

The total amount of load to be shed, ΔP^T is then calculated using equation (4-20) to be 25.55W. Since there are three loads connected to the load, the amount of power shed is divided equally among the loads. According to equation (4-21), each load is actuated so as to shed 8.52W irrespective of their individual load modes. Shedding these loads, the bus voltage is found to rise to 87.5V with the stopping criteria $|V_{TH} - V_K'| =\ 2.5V$.

Then, for the next iteration of the algorithm, V_K is updated to the new bus voltage and the load shedding is repeated. At the end of second actuation of loads, the bus voltage reaches within the tolerance limit to 88.5V and $|V_{TH} - V_K'| =\ 1.5V$. The power metric is then calculated to be 10%.

4.3.3. SCENARIO 2

In this scenario, the entire load shedding is done on only one load. In such a situation, only one of the loads has to suffer service disruption, while the other loads continue to operate at their initial values. As described below, each case evaluates the performance of the load shedding algorithm when a single load type is actuated.

Case 1. **LOAD 1 only**

$$\frac{dV}{dP1} = 0.577 \implies \Delta P = 24.78W$$

Since it is a Constant Current load with an initial load setting of 1A, initial power drawn by the load, $P_{orig} = 75.7V * 1A = 75.7W$

$P_{new} = P_{orig} - \Delta P = 75.7 - 24.78 = 50.92W$

Desired voltage, $V_{TH} = 90V \implies I_{new} = \frac{P_{new}}{V_{TH}} = 0.566A$

Dropping the load on LOAD 1 from 1A to 0.566A, while keeping the other two loads the same, $V_K' = 84.6V$ and $|V_{TH} - V_K'| = 5.4V$.

Since the stopping condition of the algorithm hasn't been met, the load shedding procedure is repeated until $|V_{TH} - V_K'|$ is within the permitted 2V tolerance. At the end of the third iteration, the bus voltage reaches 88.22V and the condition is satisfied since $|V_{TH} - V_K'| = 1.78V$. The percentage change in power is calculated as 59.2%.

Case 2.   **LOAD 2 only**

Using a similar approach as above, it was calculated that Load 2 had to drop 40.86W for the first iteration, making the new $P_{L2} = 109.14W$. So, acting on LOAD 2 while keeping the others the same first raised the bus voltage to 86.36V and $|V_{TH} - V_K'| = 3.64V$.

Further iterations are done and the load shedding is continued until at the end of the third iteration, the bus voltage reaches 88.6V and $|V_{TH} - V_K'| = 1.4V$. The power metric of percentage change in power is calculated to be 40%.

Case 3.   **LOAD 3 only**

Using similar calculations, LOAD 3 had to shed 19.01W, and it being a constant impedance load, this meant a new loading of 422.09Ω. Making this change increased the bus voltage to about 84.4V and $|V_{TH} - V_K'| = 5.6V$.

Similar to the earlier cases, the load setting of the constant impedance load is iteratively updated until the voltage of the bus is observed to be within the acceptable tolerance. At the end of third iteration, $V_K' = 88.05V$ and $|V_{TH} - V_K'| = 1.95V$. The power metric is calculated as 93%.

It is clearly seen that after just one iteration of the single load shedding algorithm, the bus voltage value is still quite far away from reaching the threshold value with $\varepsilon < 2V$ in the alternate load shedding schemes. It takes multiple repetitions of load shedding in order to increase the bus voltage to within acceptable tolerance. Moreover, the power metric value is very high – with Case 3 of Scenario 2 being the highest at 93% - indicating a steeper reduction in power drawn by the loads.

This means that in the alternate load shedding scenarios, the loads have to reduce their power usage by as much as 93% to satisfy the load shedding problem. Thus, while all load shedding algorithms are able to find a satisfactory solution, the power metric indicates larger changes in power consumed are required in the alternate scenarios than with the method proposed in this thesis.

As summarized in Table 4.2, it is observed that a parallel operation of all three loads on the bus gives the best result in terms of attaining the threshold voltage. This is an indication that actuating each of the loads according to their participation factors is the most effective way of load shedding to increase the bus voltage to the threshold value, while also maintaining minimal disruption of service to the customers connected to the bus.

Table 4.2 Summary of Results of Different Load Shedding Control Algorithms on 3 Bus Microgrid System

Control Algorithm	PROPOSED	SCENARIO 1	SCENARIO 2		
			Case 1	Case 2	Case 3
No. of loads actuated	3	3	1	1	1
No. of Iteration steps	1	2	3	3	3
$|V_{TH} - V'_K|$ (V)	1.7	1.5	1.78	1.4	1.95
Power metric (per load) (%)	8.5	10	59.2	40	93

While undergoing an increase in voltage level, the bus moves from one operating point to another in a three-dimensional space where the power consumed by each load is an independent variable. Figure 4.2 shows this during implementation of the proposed load control methodology from above on the DC bus.
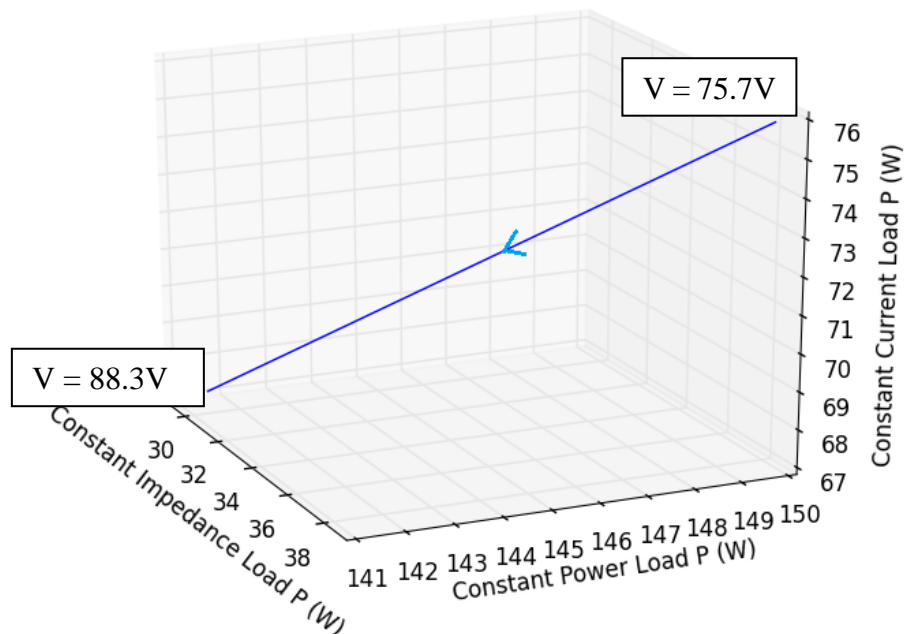
Figure 4.2 Movement of Operating Point of Bus 3 During Proposed Load Control Algorithm

In the above example, the minimum path traveled by the operating point was in the case of the proposed load control algorithm, as described in Figure 4.2. This corresponds directly to disruption in power consumed where we had an average percentage change in powers consumed by each of the three loads as 8.5% as compared to 59%, 40% and 93% for each of LOAD 1, LOAD 2 and LOAD 3 respectively, in the three individual operations of Scenario 2.

4.4. RESULTS OF LOAD SHEDDING ON THE FOUR BUS MICROGRID

The 4 bus microgrid has 2 DC buses and Loads 1 and 2 are connected to Bus 3 in operating modes of constant power 150W and constant impedance 150Ω respectively. A third load operating as a constant current load 1A is connected to Bus 4. This represents a grid structure of DC buses, both facing overloading conditions. Similar load shedding control schemes are implemented in the 4 bus microgrid testbed and some of them are presented in this section. It is to be noted that a measurement based sensitivity approach, such as the one employed in this thesis, already encapsulates the effects of the power lines between the two DC buses.

With the loads operating at their initial settings as shown in Table 4.2, both the DC buses are operating below the desired threshold voltage of 90V$_{DC}$.

Table 4.3 Initial Load Setting for the Load Shedding Problem on 4 Bus Microgrid

LOAD NUMBER	LOAD TYPE	INITIAL VALUE	BUS	COMPUTED POWER ($V_3 = 74.14\text{V}$; $V_4 = 68.86\text{V}$)
1	Constant Power	150W	3	150W
2	Constant Impedance	150Ω	3	36.64W
3	Constant Current	1A	4	68.86W

In order to obtain individual P-V curves, each of the loads are varied about +/- 10% from their average initial operating points while keeping the other loads constant. The following P-V graphs were obtained by varying each load individually on the respective buses:
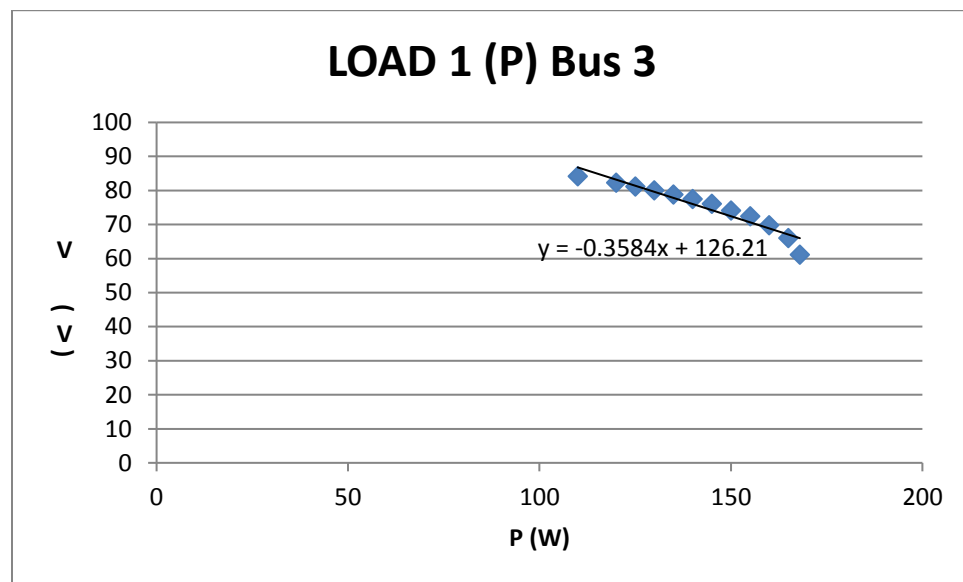
Figure 4.3 P-V Curve Obtained Varying Load 1 Keeping Other Two Fixed

LOAD 2 (Z) Bus 3

y = -0.8123x + 103.04

V (V)

P (W)
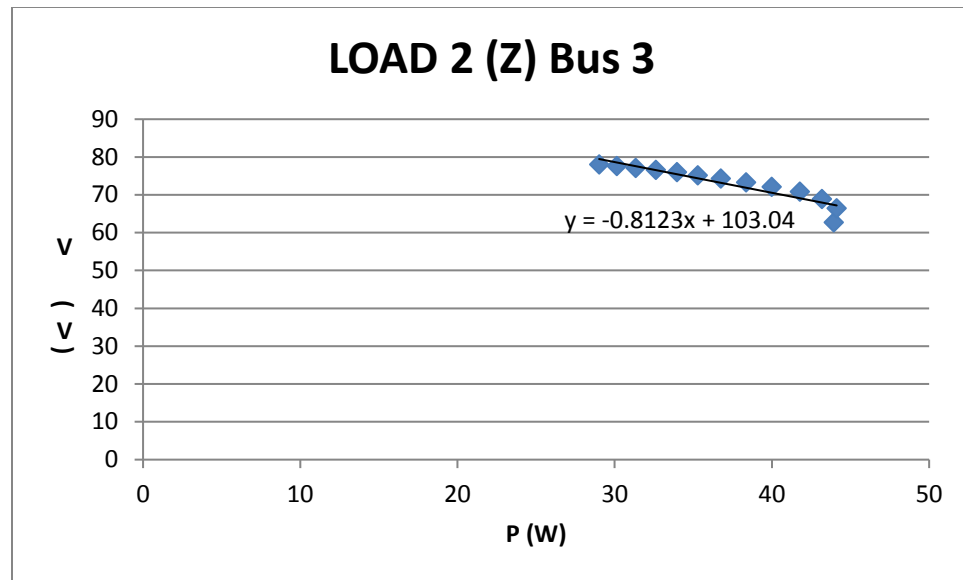
Figure 4.4 P-V Curve Obtained Varying Load 2 Keeping Other Two Fixed

LOAD 3 (I) Bus 4

y = -0.9912x + 131.86

V (V)

P (W)
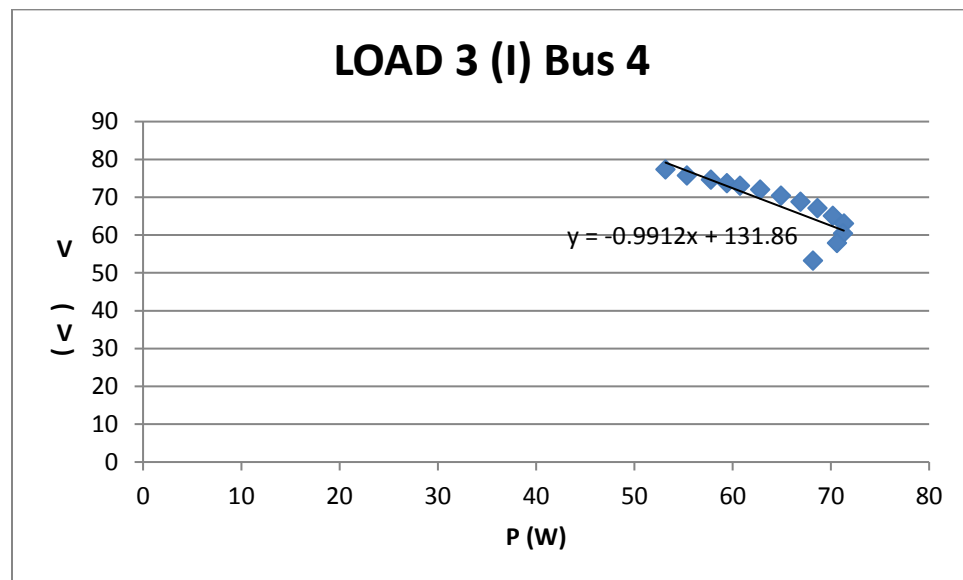
Figure 4.5 P-V Curve Obtained Varying Load 1 Keeping Other Two Fixed

This voltage sensitivity is taken to be the slope of a linear approximation of the P-V curve. The following values were obtained for each load:

$$\text{For LOAD 1 from Figure 4.3, } \frac{dV_3}{dP_1} = 0.358$$

$$\text{For LOAD 2 from Figure 4.4, } \frac{dV_3}{dP_2} = 0.812$$

$$\text{For LOAD 3 from Figure 4.5, } \frac{dV_4}{dP_3} = 0.99$$

When all the loads are operating in their constant loading values, the voltage on Bus 3 is 74.14V and the voltage on Bus 4 is 68.86V. The aim is to increase the bus voltage on each bus individually to the threshold voltage of 90V by taking control actions on the loads connected to the respective bus. No action is taken on the loads on the DC bus not under consideration in each case.

4.4.1. LOAD SHEDDING ON BUS 3

To increase the voltage on Bus 3 to 90V, from equation (4-8), $\Delta V = 15.86V$. Three different control methods are used in order to minimize the gap to the desired voltage level. The two loads connected to the bus are shed individually in turn while keeping the other at its initial value – similar to Scenario 2 in Section 4.3 - and then a third control method uses participation factors to command both the loads to shed proportionally – similar to the proposed load shedding algorithm in Section 4.3.

Case 1.   **LOAD 1 and LOAD 2 proportionally**

Using equation (4-9), the participation factors of the two loads are calculated to be:

$$\alpha_1 = 0.31$$

$$\alpha_2 = 0.69$$

The proportional power to be shed by each load is calculated using equations (4-10) and (4-11). Similar to the proposed load shedding algorithm, the equivalent load control setting is then calculated using equations (4-12) through (4-18). After calculations, LOAD 1 is set to a new operating power of $P = 136.26W$, and LOAD 2 is set to a new operating impedance of $R = 349.53\Omega$. By acting on both the loads, the voltage at Bus 3 increased to 88.2V with a $|V_{TH} - V_K'| = 1.8V$. The power metric in this case is calculated to be 12.46%. Since this attains the stopping condition in Step 4 of the proposed algorithm, load shedding can be stopped.

Case 2.   **LOAD 1 only**

Using the voltage sensitivity of LOAD 1, we get $\Delta P = 44.3W$. Since LOAD 1 is a constant power load, we change the static load value to 105.7W and find that the bus voltage rises to about 85.33V and $|V_{TH} - V_K'| = 4.67V$. The power metric is calculated to be 29.53%.

Case 3. **LOAD 2 only**

From the voltage sensitivity of LOAD 2, the required change in power is calculated as $\Delta P = 19.53W$. Since LOAD 2 is a constant impedance load, a corresponding ΔR is calculated and the equivalent impedance setting value for the load is calculated to be 473.13Ω. By changing the value of LOAD 2 while keeping LOAD 1 constant, the bus voltage increases to 83.06V and $|V_{TH} - V'_K| = 6.94V$. The power metric is calculated to be 53.28% in this case

In both Case 2 and Case 3, it is seen that the voltage difference $|V_{TH} - V'_K|$ is quite high after one iteration value. The value of the power metric is also significantly high and will only continue to increase with further iterations of the algorithm. So, it is sufficient to say that Case 1 is superior to Cases 2 and 3 and no further iterations are done.

Table 4.4 Summary of Results of Different Load Shedding Control Algorithms on Bus 3 of 4 Bus Microgrid System

Control Algorithm	CASE 1	CASE 2	CASE 3
No. of loads actuated	2	1	1
No. of Iteration steps	1	1	1
$|V_{TH} - V'_K|$ (V)	1.8	4.67	6.94
Power metric (per load) (%)	12.46	29.53	53.28

4.4.2. LOAD SHEDDING ON BUS 4

To increase voltage on Bus 4 to 90V, from equation (4-8), $\Delta V = 21.14V$. From the voltage sensitivity of the load connected to Bus 4, we get $\Delta P = 21.35W$. Since it is a constant current load, we calculate the equivalent load control setting using equations (4-12) through (4-18), and the results after actuation of the new load value is tabulated.

Table 4.5 Summary of Results of Load Shedding on Bus 4 of 4 Bus Microgrid System

Control Algorithm	CASE 1
No. of loads actuated	1
No. of Iteration steps	1
$|V_{TH} - V_K'|$ (V)	8.47
Power metric (per load) (%)	37.2

The load is seen to reduce its power consumption by 37.2% and this would only increase with further iterations of load shedding in order to reach the threshold voltage.

Hence it is seen that acting on all the loads connected to a particular bus gives the best result in terms of improving the voltage profile at the bus instead of focusing all the control actions on one load and leaving the others at its initial values.

From the results of the load shedding experiments conducted on both the 3 bus and 4 bus microgrid testbeds, summarized in Tables 4.2, 4.4 and 4.5, the proposed load control algorithm is found to be the most effective in achieving the desired voltage level in least number of iterations of load shedding. In both cases, it is also shown to have the least power metric, indicating the least disruption caused to the power consumption of the customers. Hence, it is experimentally shown that it is better for a microgrid controller to request all the customers connected to it to shed some load – both according to their load type and their participations factors – to mitigate overloading conditions.

5. CONCLUSIONS AND FUTURE WORK

5.1. CONCLUDING REMARKS

The work presented in this thesis addressed the need for a modern microgrid testbed for hybrid AC/DC distribution systems. In order to successfully operate, maintain, and upgrade the future smart grid, it is crucial to have a platform to test and validate emerging research ideas experimentally. This thesis provided such a platform in a highly reconfigurable manner to implement various AC/DC microgrid operation and control methodologies.

The major components of this testbed were:

- A programmable source capable of simulating different types of power generation such as renewable energy, storage et cetera

- Programmable loads that were operated in different load modes and operating points, having different voltage sensitivities, and therefore different reactions to the control measures applied to them

- A central remote measuring and control computer that monitored all the programmable loads and also executed the control algorithms as decided by the user.

The applications of the individual components were studied, especially the programmable loads, and its operating modes were discussed in brief. The validity of the

measurements as seen on the centralized monitoring system was also verified by comparing against the voltage and current waveforms observed on a calibrated power analyzer.

The focus was then put on using the measurements received to implement a load shedding operation. The voltage sensitivities of the individual loads connected to the DC buses were calculated, forming the basis for the control approaches experimented. It took into account different load types to demonstrate different voltage sensitivities with respect to power. A formal load shedding problem was developed, and a load control solution was proposed, to mitigate an overloading issue in the DC buses. Through testing and evaluation of results, the control strategy proposed in this thesis was found to improve the voltage profile of the buses in a more successful manner than the more traditional aggregate load control strategy used in power distribution systems, by reaching the desired threshold voltage in least number of iterations. Moreover, a power metric was introduced to compare the different solutions to the load shedding problem quantifying the percentage change in powers drawn by each of the loads.

Specific research contributions and accomplishments of the work are summarized in Section 5.2; while a future vision for the work is discussed in Section 5.3.

5.2. SUMMARY OF RESEARCH CONTRIBUTIONS

The thesis' main contributions include:

- Development of a flexible AC/DC microgrid testbed model and implementing it in a hardware experimental setup. The testbed allows for users with custom energy sources, different numbers of AC and DC buses, and different numbers of loads connected to them to conduct studies on the testbed before actually building a microgrid.

- Usage of programmable sources and loads in the laboratory testbed to emulate different types of sources and load behaviors in the microgrid.

- Expansion of the developed microgrid testbed to a larger N bus system, adding new buses through power lines and integrating them with the central monitoring and control center.

- Development of a LabVIEW-based remote monitoring and control tool that acted as the central measurement and control unit on the DC side of the microgrid testbed.

- Formulation of a load shedding problem on the DC buses of the microgrid and design of a load shedding algorithm to raise the bus voltage to within measurement tolerance of a desired threshold value.

- Investigation of the properties that distinguish between aggregate load control on a bus versus individualized load control; the properties analyzed through testing were:

  - The mode of operation of the load – namely constant current, constant power and constant resistance.

  - The dP/dV sensitivity of the load obtained through plotting a PV curve of the measurements, and hence its participation factor.

- Implementation of a load control strategy that accounted for the above stated properties of the DC loads and shed each load type in proportion to their individual participation factor. The proposed load shedding algorithm achieved a desired result in the least number of iterations of load shedding along with a minimal disruption from the initial power delivered to each of the load types – quantified by the power metric – as compared to other, more traditional, approaches to load shedding.

5.3. FUTURE WORK

Several considerations and suggestions can be made in terms of future work:

- The testbed developed in this thesis can be expanded to include more AC and DC buses by reconfiguring it and adding components in the laboratory. Necessary modifications to the LabVIEW program would also have to be done.

- Thus far, the programmable source is set to act as a constant $208V_{LL}$ source of AC power while future work on the microgrid testbed could integrate it into the central control center and use it to emulate different types of sources seen in a hybrid AC/DC microgrid.

- In a similar manner, in this thesis the loads are set to act only as constant load models. The testbed loads can also be utilized as rectified load models such as RLC mode and the behavior can be observed. Additional programmable loads can also be connected to the AC buses to give a wider scope of research on the testbed.

- Alternative solutions to the overloading problem presented in Chapter 4 can be investigated. Other approaches can include solving the heavy loading issue by source voltage regulation. However, care has to be taken to avoid exceeding the maximum power handling capacity of the source.

- Since the proposed load shedding control was optimal compared to the other alternate solutions, an automated controller that uses this algorithm can be integrated into the central measurement and control environment. This would decrease the response time to unstable conditions on the microgrid and thus improve overall quality of service to the loads connected to the microgrid testbed.

- Additional research on the converter that interfaces the DC sub-grid to the AC sub-grid is an open topic. Use of bidirectional interlinking converters can allow flow of power in both directions that can open doors to more complex control methods on the microgrid.

- Since the measurements are received on a computer, they can be transmitted wirelessly to another computer representing a remote control center in, for instance, a shipboard power system. Analytical study of the delays in receiving measurements at the remote center can give an understanding of possibility of wireless communication in a microgrid system. Once the measurement delays are comprehended, closing the loop to implement control can be investigated.

LIST OF REFERENCES

1. S. Carullo and C. O. Nwankpa, "Interconnected power systems laboratory: a computer automated instructional facility for power system experiments," IEEE Trans. Power Syst., vol. 17, no. 2, pp. 215–222, May 2002

2. Carullo, Stephen P., and Chika O. Nwankpa. "Experimental validation of a model for an information-embedded power system." *IEEE Transactions on Power Delivery* 20.3 (2005): 1853-1863.

3. Aravinthan, Visvakumar, et al. "Wireless communication for smart grid applications at distribution level—Feasibility and requirements." *Power and Energy Society General Meeting, 2011 IEEE*. IEEE, 2011.

4. Schonberger, John, Simon Round, and Richard Duke. "Autonomous load shedding in a nanogrid using DC bus signalling." *IEEE Industrial Electronics, IECON 2006-32nd Annual Conference on*. IEEE, 2006.

5. Miu, Karen, et al. "Testing of shipboard power systems: a case for remote testing and measurement." *Electric Ship Technologies Symposium, 2005 IEEE*. IEEE, 2005.

6. Model, Chroma. "63800 Series Programmable AC/DC Electronic Load."

7. Otomega, Bogdan, Mevludin Glavic, and Thierry Van Cutsem. "Distributed undervoltage load shedding." *IEEE Transactions on Power Systems* 22.4 (2007): 2283-2284.

8. Zubieta, Luis Eduardo. "Are microgrids the future of energy?: Dc microgrids from concept to demonstration to deployment." *IEEE Electrification Magazine* 4.2 (2016): 37-44.

9. Ton, Dan T., and Merrill A. Smith. "The US Department of Energy's microgrid initiative." *The Electricity Journal* 25.8 (2012): 84-94.

10. Wang, Peng, et al. "Harmonizing AC and DC: A hybrid AC/DC future grid solution." *IEEE Power and Energy Magazine* 11.3 (2013): 76-83.

11. Wang, Peng, et al. "Hybrid AC/DC Micro-Grids: Solution for High Efficient Future Power Systems." *Sustainable Power Systems*. Springer Singapore, 2017. 23-40.

12. Lasseter, Robert H., and Paolo Paigi. "Microgrid: A conceptual solution." *Power Electronics Specialists Conference, 2004. PESC 04. 2004 IEEE 35th Annual*. Vol. 6. IEEE, 2004.

13. Saleh, Mahmoud, et al. "Design and implementation of CCNY DC microgrid testbed." *Industry Applications Society Annual Meeting, 2016 IEEE*. IEEE, 2016.

14. Lobo, Joyer Benedict, and Peter Idowu. "Laboratory scale microgrid test bed: Hardware implementation." *10th CMU workshop for smart grid testbed*. 2015.

15. Li, Hua, et al. "The generation of ZIP-V curves for tracing power system steady state stationary behavior due to load and generation variations." *Power Engineering Society Summer Meeting, 1999. IEEE*. Vol. 2. IEEE, 1999.

16. Majumder, Ritwik. "Some aspects of stability in microgrids." *IEEE Transactions on power systems* 28.3 (2013): 3243-3252.

17. Guerrero, Josep M., et al. "Advanced control architectures for intelligent microgrids—Part I: Decentralized and hierarchical control." *IEEE Transactions on Industrial Electronics* 60.4 (2013): 1254-1262.

18. Kwasinski, Alexis, and Chimaobi N. Onwuchekwa. "Dynamic behavior and stabilization of DC microgrids with instantaneous constant-power loads." *IEEE Transactions on Power Electronics* 26.3 (2011): 822-834.

19. Kundur, Prabha, Neal J. Balu, and Mark G. Lauby. *Power system stability and control*. Vol. 7. New York: McGraw-hill, 1994.

20. Tong, Shiqiong. "Participation factor studies for distributed slack bus models in three-phase distribution power flow analysis." *Transmission and Distribution Conference and Exhibition, 2005/2006 IEEE PES*. IEEE, 2006.

21. Wang, Peng, et al. "A hybrid AC/DC micro-grid architecture, operation and control." *Power and Energy Society General Meeting, 2011 IEEE*. IEEE, 2011.

22. Lantero, Allison. "The War of the Currents: AC vs. DC Power." *Washington DC, Energy. Gov* (2013).

23. Lidula, N. W. A., and A. D. Rajapakse. "Microgrids research: A review of experimental microgrids and test systems." *Renewable and Sustainable Energy Reviews* 15.1 (2011): 186-202.

24. Hossain, Eklas, et al. "Microgrid testbeds around the world: State of art." *Energy Conversion and Management* 86 (2014): 132-153.

25. Ustun, Taha Selim, Cagil Ozansoy, and Aladin Zayegh. "Recent developments in microgrids and example cases around the world—A review." *Renewable and Sustainable Energy Reviews* 15.8 (2011): 4030-4041.

26. Bhaskara, Shyam Naren, and Badrul H. Chowdhury. "Microgrids—A review of modeling, control, protection, simulation and future potential." *Power and Energy Society General Meeting, 2012 IEEE*. IEEE, 2012.

27. Kakigano, Hiroaki, Yushi Miura, and Toshifumi Ise. "Low-voltage bipolar-type DC microgrid for super high quality distribution." *IEEE transactions on power electronics* 25.12 (2010): 3066-3075.

28. Lasseter, Robert H., et al. "CERTS microgrid laboratory test bed." *IEEE Transactions on Power Delivery* 26.1 (2011): 325-332.

29. Hossain, Eklas, et al. "Microgrid facility around Asia and far east." *Renewable Energy Research and Application (ICRERA), 2014 International Conference on*. IEEE, 2014.

30. Haidar, Ahmed MA, Kashem Muttaqi, and Danny Sutanto. "Smart Grid and its future perspectives in Australia." *Renewable and Sustainable Energy Reviews* 51 (2015): 1375-1389.

31. Bayindir, Ramazan, et al. "Microgrid facility at European union." *Renewable Energy Research and Application (ICRERA), 2014 International Conference on*. IEEE, 2014.

32. International Energy Agency. "*World Energy Outlook 2017.*"

APPENDIX A: LIST OF NOMENCLATURE

In order of appearance:

N	number of buses in the microgrid system
V_{dc}	DC voltage
V_{LL}	line-to-line voltage
V_K	voltage at bus K
V_{TH}	desired threshold voltage at a bus
P_{DC}	average DC power consumed by a load connected to the bus
P_{nom}	nominal power value of the constant power load
I_{nom}	nominal current value of the constant current load
R_{nom}	nominal resistance value of the constant impedance load
V_K'	voltage at bus K after implementation of load control
ε	allowable difference from threshold voltage due to noise in measurement
X, Y, Z	average DC power consumed by each of the three loads connected to a bus
α	participation factor of each load in load shedding algorithm
ΔP_i^T	total power to be shed by load i to meet load shedding requirement
ΔP_i	participation factor dependent amount of power to be shed by load i
$I_{nom}, P_{nom},$ R_{nom}	original setpoints of the three loads
$I_{new}, P_{new},$ R_{new}	new controller setpoints of the three loads
P_{orig}, P_{new}	average DC power consumed by each load before and after actuation to new controller setpoints

APPENDIX B: OPERATING INSTRUCTIONS FOR THE TESTBED

Once the AC/DC microgrid testbed has been setup and connections are done according to the circuit diagram in Chapter 2 (Figure 2.2 for 3 bus system and Figure 2.4 for 4 bus system), the procedure to have it functional for load control through the software interface is explained as follows:

1. Switch ON the power supply to the programmable source and loads and allow the device an initialization time to run customary self-diagnostic tests.
2. Choose AC coupling mode on the programmable source and set the phase voltage value of each phase as 120V, without triggering the output of the source. The output setting can also be saved as a custom setting for recall upon restart.
3. Launch the LabVIEW based measurement and control unit on the computer to which the three loads and the Yokogawa scope have been connected to through GPIB cables.
4. Select the unique GPIB addresses assigned to each device from the drop-down menu in its respective initialization window as seen in Figure 3.5. The initialization window of the Yokogawa scope is shown in Figure B.1. Once it is initialized through a unique GPIB address, the data update rate is set within an interval range of 50ms and 20s. To get the time/div setting, the update interval is divided by 10 since 10 divisions can be viewed on the scope. The data acquisition time for the waveform is then set as the time/division setting. The user can also initialize the FFT settings for viewing harmonics, though that feature was beyond the scope of this thesis. Once initialization is complete, run the LabVIEW code to activate remote monitoring and control of the loads.
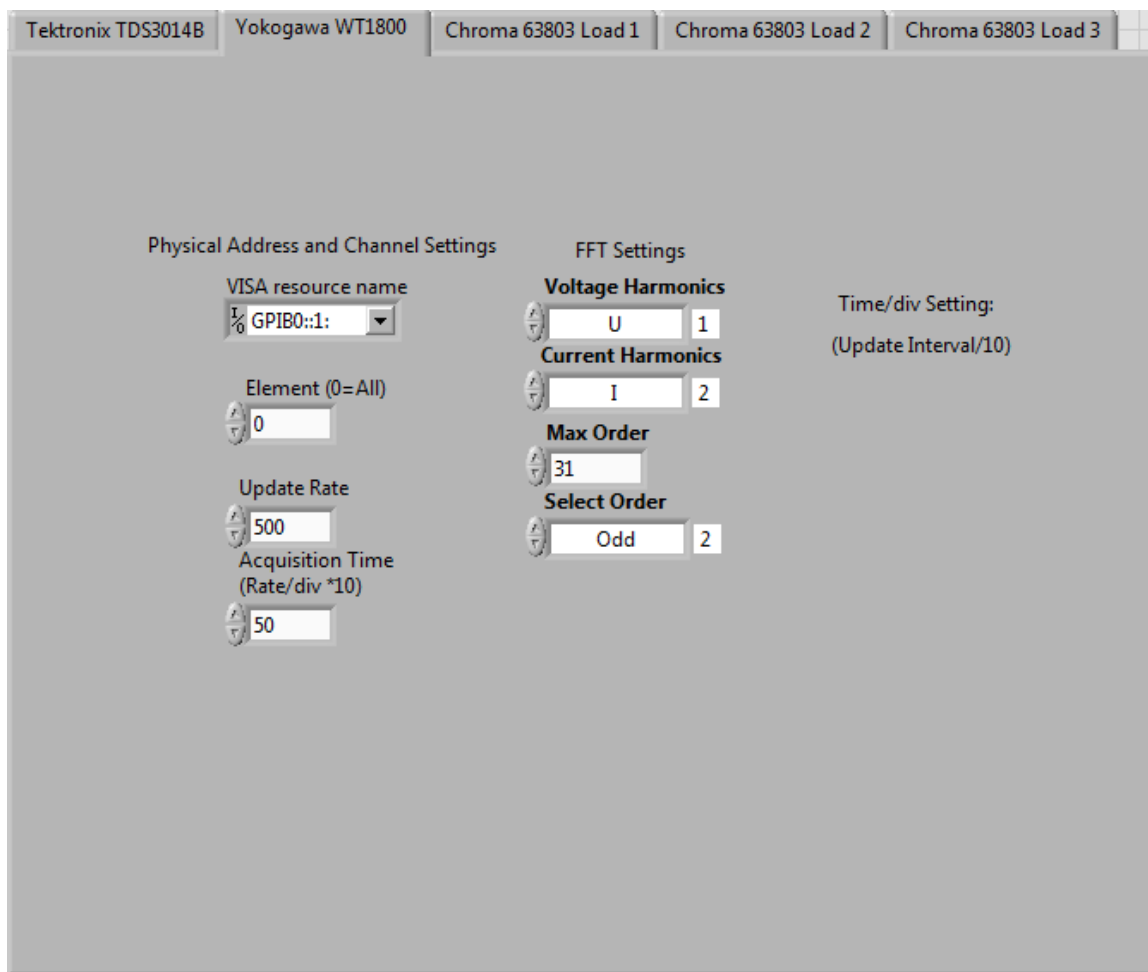
| Tektronix TDS3014B | Yokogawa WT1800 | Chroma 63803 Load 1 | Chroma 63803 Load 2 | Chroma 63803 Load 3 |

Physical Address and Channel Settings

VISA resource name
GPIB0::1:

Element (0=All)
0

Update Rate
500

Acquisition Time
(Rate/div *10)
50

FFT Settings

Voltage Harmonics
U   1

Current Harmonics
I   2

Max Order
31

Select Order
Odd   2

Time/div Setting:

(Update Interval/10)

Figure B.1 Initialization Window of Yokogawa Power Analyzer

5. Trigger the output of the programmable source (visible as the blue button in Figure 2.6) to power the microgrid testbed.

6. Slowly increase the autotransformer tap setting to increase the DC voltage at Bus 3 to 120V by continuously observing the voltage level on the load measurement window as seen in Figure 3.7. Once it is set, keep the source and autotransformer setting fixed throughout the experiment.

7. Now, in the initialization window of each load, select DC mode of operation and select the load simulation mode from the drop-down menu – selecting a different ZIP load mode for each of the loads.

8. It can be seen that corresponding load parameter setting windows are accessible in the respective load control windows while the other parameter settings are blocked out as shown in Figure 3.6.

9. First and foremost, the protective current for each load is set as 12A to limit the maximum amount of current flowing upstream. The settings can be implemented by hitting the Enter button on the keyboard.

10. Now for each of the loads, desired setpoints are set on the controller. The loads can then be triggered ON or kept OFF as desired.

11. The load measurements can be viewed simultaneously on the measurement window and verified through the Yokogawa power analyzer measurements. Figure B.2 shows a screenshot of the measurement window seen on the LabVIEW program while the power is OFF.

Measurement Name		Element Number					
		1	2	3	4	5	6
Urms	0	0	0	0	0	0	0
Irms	0	0	0	0	0	0	0
S		0	0	0	0	0	0
P		0	0	0	0	0	0
Q		0	0	0	0	0	0
PF		0	0	0	0	0	0
PF Angle		0	0	0	0	0	0
THD P		0	0	0	0	0	0
THD U		0	0	0	0	0	0
THD I		0	0	0	0	0	0

Figure B.2 Screenshot of the Yokogawa Power Analyzer Measurement Window

12. The controller setpoints can also be changed while the loads are ON by entering a new value and hitting the Enter button. However, care is to be taken that the load settings do not drive the bus voltage below the programmable load's operating range of 50-350V.

13. If the programmable load trips for any reason, turn the load state OFF for each load, stop the execution of the LabVIEW code and manually clear the error on the face of the load. Once the error is cleared, the code can be restarted keeping earlier initializations.

14. Once desired load control studies have been performed, turn each of the load states to OFF and stop the Lab VIEW code execution.

15. Slowly decrease the autotransformer back to zero. Trigger OFF the output of the programmable source before switching off the source.